NAVAL POSTGRADUATE SCHOOL
Monterey, California

THESIS

DESIGN AND CONSTRUCTION OF AN EXPANDABLE SERIES TRANS-AUGMENTED ELECTROMAGNETIC RAILGUN

by

Michael R. Lockwood

June 1999

Thesis Advisor: William B. Maier II
Co-Advisor: Andres Larazza

Approved for public release; distribution is unlimited.

REPORT DOCUMENTATION PAGE

Form Approved OMB No. 0704-0188

1. AGENCY USE ONLY *(Leave blank)*	2. REPORT DATE June 1999	3. REPORT TYPE AND DATES COVERED Master's Thesis

4. TITLE AND SUBTITLE Design and Construction of an Expandable Series Trans-augmented Electromagnetic Railgun

5. FUNDING NUMBERS

6. AUTHOR(S)
Lockwood, Michael R.

7. PERFORMING ORGANIZATION NAME(S) AND ADDRESS(ES)
Naval Postgraduate School
Monterey, CA 93943-5000

8. PERFORMING ORGANIZATION REPORT NUMBER

9. SPONSORING / MONITORING AGENCY NAME(S) AND ADDRESS(ES)

10. SPONSORING / MONITORING AGENCY REPORT NUMBER

11. SUPPLEMENTARY NOTES
The views expressed in this thesis are those of the author and do not reflect the official policy or position of the Department of Defense or the U.S. Government.

12a. DISTRIBUTION / AVAILABILITY STATEMENT
Approved for public release; distribution is unlimited.

12b. DISTRIBUTION CODE

13. ABSTRACT *(maximum 200 words)*

Long range maritime land attack can be accomplished with today's chemically propelled munitions only by sacrificing responsiveness. Projectiles launched with electromagnetic forces can achieve velocities above 2-3 kilometers per second. The technical challenges to be overcome before electromagnetic launch can be considered practical for maritime land attack include development of high density pulsed power supplies, high current power switching and a long life launcher. To investigate electromagnetic launch technology a 1.2 meter railgun was constructed. It was designed to allow augmentation and various bore configurations. The railgun power unit consists of two 11 kV, 830μf capacitors discharging through a 7μH inductor coil. A crowbar circuit provides capacitor protection. Operational testing of the firing circuit, instrumentation, power unit, and launcher structure was satisfactory. The 7μH coil induced currents within the power unit, which adversely effected triggering circuitry. The molybdenum projectiles initially tested proved disappointing due to their tendency to meld with the copper rails. An extended current pulse resulting from such a meld caused failure of the crowbar circuit, which curtailed further testing. The induction coil could safely be discarded, and a revised crowbar circuit will prevent further failure. Future operational testing will focus on alternative armature materials and designs and on operational methods.

14. SUBJECT TERMS
Electromagnetic Railgun, Electromagnetic Launch, Railgun Augmentation

15. NUMBER OF PAGES
62

16. PRICE CODE

17. SECURITY CLASSIFICATION OF REPORT	18. SECURITY CLASSIFICATION OF THIS PAGE	19. SECURITY CLASSIFI- CATION OF ABSTRACT	20. LIMITATION OF ABSTRACT
Unclassified	Unclassified	Unclassified	UL

NSN 7540-01-280-5500

Standard Form 298 (Rev. 2-89)
Prescribed by ANSI Std. 239-18 298-102

DESIGN AND CONSTRUCTION OF AN EXPANDABLE SERIES TRANS-AUGMENTED ELECTROMAGNETIC RAILGUN

Michael R. Lockwood
Lieutenant, United States Navy
B.S.M.E., Rochester Institute of Technology, 1991

Submitted in partial fulfillment of the
requirements for the degree of

MASTER OF SCIENCE IN APPLIED PHYSICS

From the

NAVAL POSTGRADUATE SCHOOL

June 1999

Author: ______________________
Michael R. Lockwood

Approved by: ______________________
William B. Maier II, Thesis Advisor

____
Andres Larraza, Co-Advisor

____
William B. Maier II, Chairman
Department of Physics

ABSTRACT

Long range maritime land attack can be accomplished with today's chemically propelled munitions only by sacrificing responsiveness. Projectiles launched with electromagnetic forces can achieve velocities above 2-3 kilometers per second. The technical challenges to be overcome before electromagnetic launch can be considered practical for maritime land attack include development of high density pulsed power supplies, high current power switching and a long life launcher. To investigate electromagnetic launch technology a 1.2 meter railgun was constructed. It was designed to allow augmentation and various bore configurations. The railgun power unit consists of two 11 kV, 830μf capacitors discharging through a 7μH inductor coil. A crowbar circuit provides capacitor protection. Operational testing of the firing circuit, instrumentation, power unit, and launcher structure was satisfactory. The 7μH coil induced currents within the power unit, which adversely effected triggering circuitry. The molybdenum projectiles initially tested proved disappointing due to their tendency to meld with the copper rails. An extended current pulse resulting from such a meld caused failure of the crowbar circuit, which curtailed further testing. The induction coil could safely be discarded, and a revised crowbar circuit will prevent further failure. Future operational testing will focus on alternative armature materials and designs and on operational methods.

TABLE OF CONTENTS

ACKNOWLEDGEMENT

I am grateful for the support from the Naval Postgraduate School on this work. I would also like to thank W. B. Maier II for his technical assistance and guidance. The expert machining services and insightful suggestions of Gary Beck were instrumental in the construction and maintenance of the gun. My deepest appreciation goes to Don Snyder who truly made everything happen. From design to construction to testing he was there every step of the way with timely advice, tremendous hard work and patience.

I. INTRODUCTION

A. HISTORY

Electromagnetic launch (EML) is the "acceleration of an object by electromagnetic forces along a guideway to initiate subsequent flight."[1]

Electromagnetic launchers have been studied for over 90 years, with 45 patents issued before the Second World War. One of the earliest examples of EML was the "Patent Electric Cannon" developed by Birkeland in 1901. The book *Cannons Electrique*, was published by Fauchon-Villeplee in 1920 and there are examples of German and Japanese EML research during the Second World War. In the 1950's EML research was sponsored by both the US Navy and Air Force [2].

The first major breakthrough was achieved at the Australian National University by Richard Marshal and his colleagues when they accelerated a 3 gram projectile in an evacuated gun system to almost 6 kilometers per second with a plasma arc [3].

In 1992 the US Army initiated a comprehensive Focused Technology program with the University of Texas. The Center for Electromechanics (CEM-UT) was formed to take the lead in research and development [4]. Presently, the majority of the EML work being done in the United States is concentrated at CEM-UT.

In 1998 the Director, Test and Evaluation and Technology Requirements (N091) asked the Center for Naval Analyses (CNA) to assess the status of railgun technology and its applicability to the surface ship land attack mission. CNA found that while there were no physics limitations that would prevent the achievement of energies at the required levels there were formidable engineering challenges. CNA recommended that, "... the Navy pursue basic railgun technology and provide modest funding to support a more detailed analytical study by the Navy's technical community".[5]

B. THE CASE FOR ELECTROMAGNETIC RAILGUNS

"The lack of an all-weather 24-hour fire support capability becomes more significant with the current focus on operations in littoral regions and the development of amphibious operations from over-the-horizon. The immediate "remedy" for this situation, the five-inch Extended Range Guided Munitions (ERGM) program, in the opinion of many naval experts, is all smoke and mirrors." [6]

The emergence of Naval Surface Fires as a major mission arena for the U.S. Navy must be shaped by the tactical requirements of the forces ashore. According to the Marine Corps doctrine supporting fires must cover the littoral area loosely defined as up to 200 nautical miles inland, be capable of a large volume of accurate fire, and provide timely response to tactical requests, on the order of two-minutes and 30 seconds [6].

The range and responsiveness of conventional propellant guns is ultimately limited by the theoretical maximum muzzle velocity. This velocity depends on the speed of sound in the expanding chemical explosives, which is about 5900 ft/s or 1.8 km/s [7]. This theoretical maximum is not approached by ERGM, which has a muzzle velocity of 2900 ft/s or 0.88 km/s. Moreover, ERGM uses a solid rocket sustainer to achieve its maximum range of 63 nm with a time of flight of seven minutes. Also, due to the size of the projectile/rocket motor/powder unit, weapon capacity is limited to 230 ERGM rounds per magazine [6].

Recalling the tactical requirements of forces ashore, it is clear that ERGM fails in range, responsiveness and volume of fire. In contrast, electromagnetic gun technology suffers from no theoretical limitations to achievable velocity. Velocities approaching 10 km/s or 33,000 ft/s have been achieved in the laboratory [8]. However, velocities above 3 km/s (9800 ft/s) are probably not useful within the atmosphere.

High velocity is necessary to achieve the responsiveness and range required. A tactically significant mass, say 50 kg (about 110 lbs.), could theoretically be launched from an electromagnetic gun out to 220 nautical miles with a muzzle velocity of 2 km/s or about 6500 ft/s [5].

Other advantages of electromagnetic guns are ease of integration with future naval vessels for which electric drive systems are anticipated. Magazine capacity two or three times that for ERGM, for the same volume could be anticipated [9]. This would be due to elimination of propellant and rocket motor from the ammunition loadout.

C. CURRENT TECHNOLOGICAL LIMITATIONS

While the potential advantages of Electromagnetic guns for Naval Surface Fire Support are impressive there are four major areas which pose technical challenges which must be overcome before railguns may be seen as practical weapons. These are: Pulsed Power Supply Thermal Management, High Current Switching Systems, High Velocity Projectile Design and Railgun barrel life [9].

Prime power sources for a railgun pulsed power supply are capacitors or compulsators. Large capacitor banks typically have low energy density with respect to both volume and weight. Conversely compensated pulsed alternators or compulsators have much higher energy densities and high efficiency. For a railgun firing a 50 kg projectile to 3 km/s about 1.44 GJ of pulsed power would be required. This translates to a volume of about 180 m^3 for a compulsator type power unit [5]. This represents about 5% of the volume occupied by conventional propellants in a modern warship.

D. PROJECT OBJECTIVE

The goal of this railgun project is to design and build a railgun capable of launching projectiles of various masses, materials and configurations, in a safe and reliable manner, to velocities of a few kilometers per second. This railgun will support research into rail longevity issues, armature and projectile design, and railgun efficiency.

II. THEORY

A. FORCE

As shown in Figure 2.1, the simple railgun consists of two parallel conductors with a conducting armature between them. A current, I, traveling through the rails induces a magnetic field, B, between them. The interaction of the armature current with the magnetic field induces an electromagnetic force called the Lorentz force.

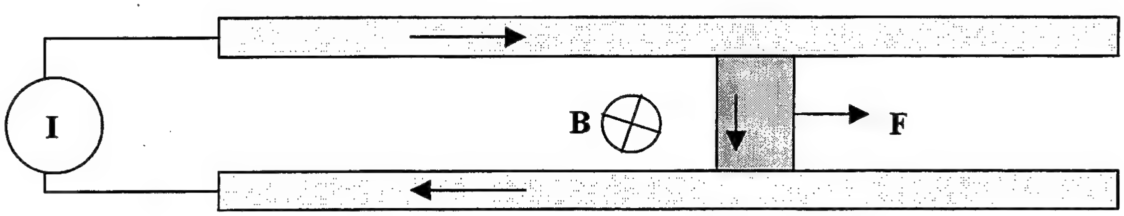

Figure 2.1 Simple Railgun.

Projectiles are accelerated by the Lorentz Force:

$$\vec{F} = q\vec{v}_d \times \vec{B} \tag{2.1}$$

where q is charge, $\vec{v}_d$ is the drift velocity of that charge through the armature and $\vec{B}$ is the magnetic field between the rails.

The magnitude of the Lorentz force is then,

$$F = qv_d B \tag{2.2}$$

where $|\vec{v}_d| = v_d$, and $|\vec{B}| = \vec{B}$.

Now,

$$q = (I)(t) = I\left(\frac{l}{v_d}\right),$$

$$dq = Idt = I\left(\frac{dx}{v_d}\right)$$

where I is the current through the armature, l is the distance between the rails and dx is an infinitesimal increment of that distance.

So,

$$dF = (dq)v_d B = BIdx \tag{2.3}$$

To find the magnetic field, B, we begin with the magnetic field for a long straight wire,

$$B_w = \frac{\mu_0 I}{2\pi\, r} \tag{2.4}$$

where μ_0 is the permeability constant and r is the radial distance from the center of the wire.

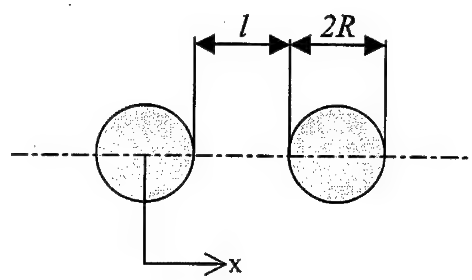

Figure 2.2 Two long straight wires.

For two parallel long straight wires, Fig. 2.2, each with a radius of R, separated by a distance l, with the origin at the center of one of the rails, the Lorentz force between them is:

$$F = \frac{\mu_0 I^2}{2\pi}\int_R^{R+l}\left[\left(\frac{1}{x}\right)+\left(\frac{1}{2R+l-x}\right)\right]dx$$

So,

$$F = \frac{\mu_0 I^2}{2\pi}\left[\ln\left(\frac{R+l}{R}\right) - \ln\left(\frac{R}{R+l}\right)\right] = \frac{\mu_0 I^2}{2\pi}\ln\left[\frac{(R+l)^2}{R^2}\right]$$

The term,

$$L' \equiv \frac{\mu_0}{\pi}\ln\left(\frac{(R+l)^2}{R^2}\right)$$

with the dimensions, $\left(\frac{tesla \cdot meter}{Ampere}\right)$ or $\left(\frac{henries}{meter}\right)$, is known as the inductance gradient.

So, the final form of the magnitude of the Lorentz force is expressed as

$$F = \tfrac{1}{2}L' I^2 \tag{2.5}$$

The equation of motion for the railgun projectile within the bore is then:

$$F = ma = \tfrac{1}{2}L' I^2 - k_f v - \tfrac{1}{2}CAv^2\rho$$

where the $k_f v$ term represents surface frictional loss and the $\frac{1}{2}CAv^2\rho$ term represents loss due to air drag. If $k_f v << \frac{1}{2}CAv^2\rho$, then

$$ma = m\frac{dv}{dt} = m\frac{dv}{dt}\frac{dx}{dx} = mv\frac{dv}{dx} = \tfrac{1}{2}L' I^2 - \tfrac{1}{2}CAv^2\rho \tag{2.6}$$

So, recalling $d(v^2) = 2vdv$, and setting $\alpha = \frac{1}{2}CA\rho$,

$$\frac{mvdv}{\frac{1}{2}L' I^2 - v^2\alpha} = dx \Rightarrow \frac{md(v^2)}{2\left(\frac{1}{2}L' I^2 - v^2\alpha\right)} = dx$$

Recalling

$$\int \frac{dx}{(a+bx)} = \tfrac{1}{b}\ln(a+bx)$$

We find,

$$\frac{-m}{2\alpha}\ln\tfrac{1}{2}\left(L'I^2 - v^2\alpha\right) = x + K$$

At $x = 0, v = 0$,

$$K = \frac{-m}{2\alpha}\ln\left(\tfrac{1}{2}L'I^2\right)$$

So,

$$x - \frac{m}{2\alpha}\ln\left(\tfrac{1}{2}L'I^2\right) = \frac{-m}{2\alpha}\ln\left(\tfrac{1}{2}L'I^2 - v^2\alpha\right)$$

Solving for x,

$$x = \frac{-m}{2\alpha}\left[\ln\left(\tfrac{1}{2}L'I^2 - v^2\alpha\right) - \ln\left(\tfrac{1}{2}L'I^2\right)\right]$$

$$x = \frac{-m}{2\alpha}\ln\left(1 - \frac{2v^2\alpha}{L'I^2}\right) \tag{2.7}$$

Now,

$$\frac{-2x\alpha}{m} = \ln\left(1 - \frac{2v^2\alpha}{L'I^2}\right)$$

Exponentiating,

$$e^{-2x\alpha/m} = \left(1 - \frac{2v^2\alpha}{L'I^2}\right)$$

Solving for v,

$$v^2 = \frac{L'I^2}{2\alpha}\left(1 - e^{-2x\alpha/m}\right)$$

$$v = \left[\frac{L'I^2}{2\alpha}\left(1 - e^{-2x\alpha/m}\right)\right]^{\frac{1}{2}} \tag{2.8}$$

This formula can be used to estimate the muzzle velocity for a specific railgun, provided that the frictional losses in surface contact are small.

B. GUN AUGMENTATION

Considering equation (2.5), for the Lorentz force:

$$F = \tfrac{1}{2}L'I^2 \tag{2.5}$$

It is clear that the force generated by a railgun can be increased by either increasing the current, which provides a force increase proportional to square of the current, I, or by augmenting the magnetic field of the gun, thus increasing inductance gradient, L'. This augmentation can be accomplished two ways; permanent magnets and trans-augmentation.

The installation of permanent magnets aligned to augment the induced magnetic field in the bore, as seen in Fig. 2.3, can substantially improve performance.

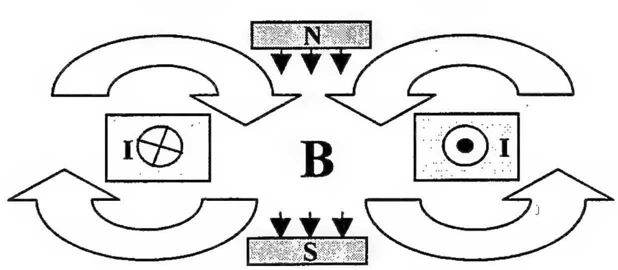

Figure 2.3 Permanent Magnet Augmentation.

With this augmentation the force on the armature is:

$$F = \tfrac{1}{2} L' I^2 + B_0 h I \tag{2.9}$$

where B_0 is the magnetic field of the permanent magnets and h is the distance between the rails [10].

Similarly, in trans-augmentation an induced magnetic field from a second set of conductors, parallel to the primary set, supplements the magnetic field in the bore. The augmentation rails can be placed in either electrical parallel or series with the primary rails as shown in Figs. 2.4 and 2.5.

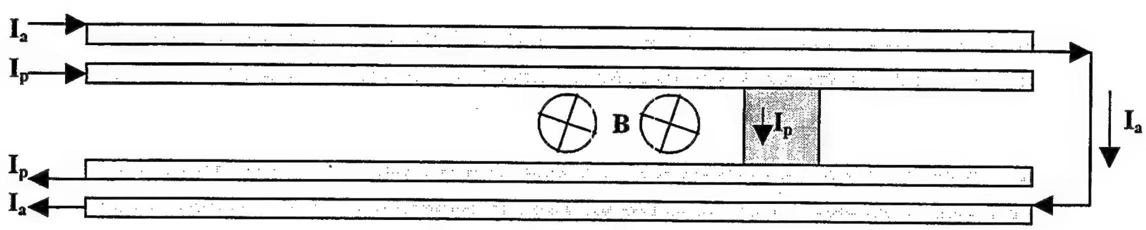

Figure 2.4 Parallel trans-augmented railgun.

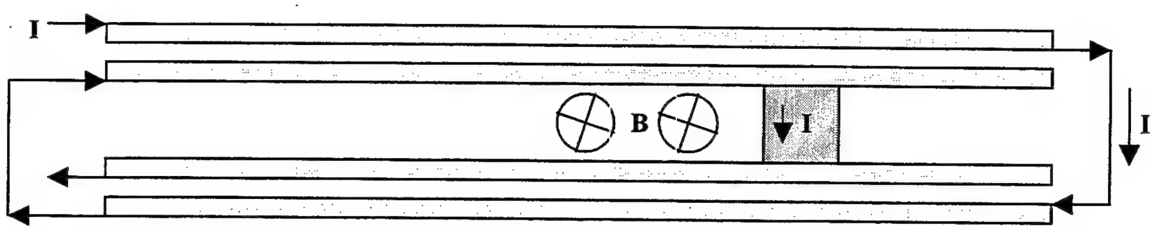

Figure 2.5 Series trans-augmented railgun.

The force equation for a trans-augmented railgun is the same as equation (2.1) except the inductance gradient increases:

$$F = \tfrac{1}{2} L'_a I^2 \tag{2.10}$$

where L'_a is the augmented inductance gradient, such that $L'_a > L'$.

The magnitude of this augmented inductance gradient can be estimated. Beginning with (2.3) and (2.4), and assuming the currents travel down the middle of the rails, the magnitude of the Lorentz force for the configuration shown in Fig. 2.6 is:

$$F=\frac{\mu_0 I^2}{2\pi}\int_{R}^{3R}\left[\left(\frac{1}{x}\right)+\left(\frac{1}{4R-x}\right)+\left(\frac{1}{\frac{5}{2}R+x}\right)+\left(\frac{1}{\frac{13}{2}R-x}\right)\right]dx$$

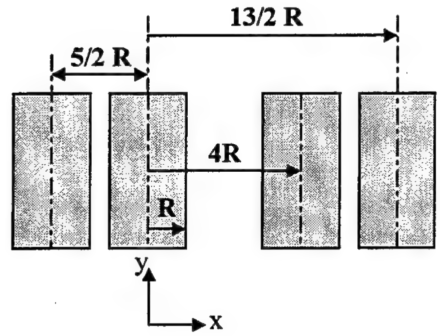

Figure 2.6 Rail configuration for augmentation estimate.

integrating,

$$F=\frac{\mu_0 I^2}{2\pi}\left[\ln\left(\frac{3R}{R}\right)+\ln\left(\frac{3R}{R}\right)+\ln\left(\frac{\frac{11}{2}R}{\frac{7}{2}R}\right)+\ln\left(\frac{\frac{11}{2}R}{\frac{7}{2}R}\right)\right]$$

and,

$$F=\frac{\mu_0 I^2}{2\pi}\left[\ln(3)+\ln(3)+\ln(\tfrac{11}{7})+\ln(\tfrac{11}{7})\right]=\frac{\mu_0 I^2}{2\pi}(2.198+0.904)$$

Now,

$$\frac{L'_a}{L'}=\frac{2.198+0.904}{2.198}=1.41 \qquad (2.11)$$

So, the augmented inductance gradient is 41% greater than the un-augmented inductance gradient, for this configuration.

III. RAILGUN DESIGN

A. POWER UNIT DESIGN

A previous railgun power supply developed at Naval Postgraduate School was analyzed prior to designing our power unit. This apparatus' characteristics were rugged simplicity and maximum use of available components. This power supply used four 100 µf, 10 kV, high-energy capacitors providing 20kJ of energy. Main power switching was accomplished with a TVS-40 vacuum switch capable of operating up to 20kV and 100kA [11].

While operationally extremely successful and efficient, this power supply configuration produced an under-damped, rapidly oscillating output, Fig. 3.1. Repeated

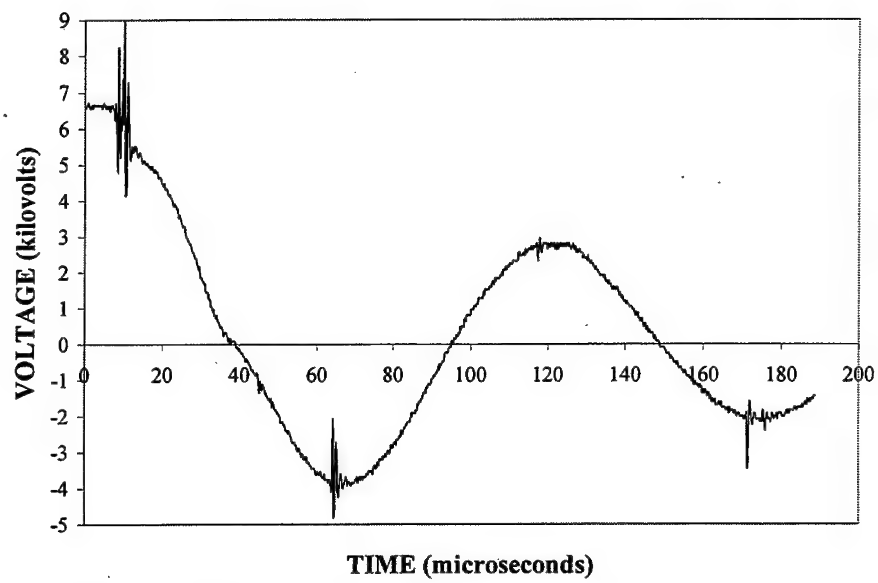

Figure 3.1 Underdamped railgun power supply discharge.

firing caused damage to the capacitors due to reverse charging [11].

To prevent oscillation, our power unit design, Fig. 3.2, crowbars the capacitors when the current has reached its peak value, thus extending the high current portion of the output pulse. The crowbar action is accomplished by a string of DA24 F2003 high power avalanche diodes, from ABB Semiconductors AG of Lenzburg, Switzerland.

Since each diode could stand off 2000 VDC, six diodes were required in each diode string to hold off the maximum capacitor potential of 11 kV.

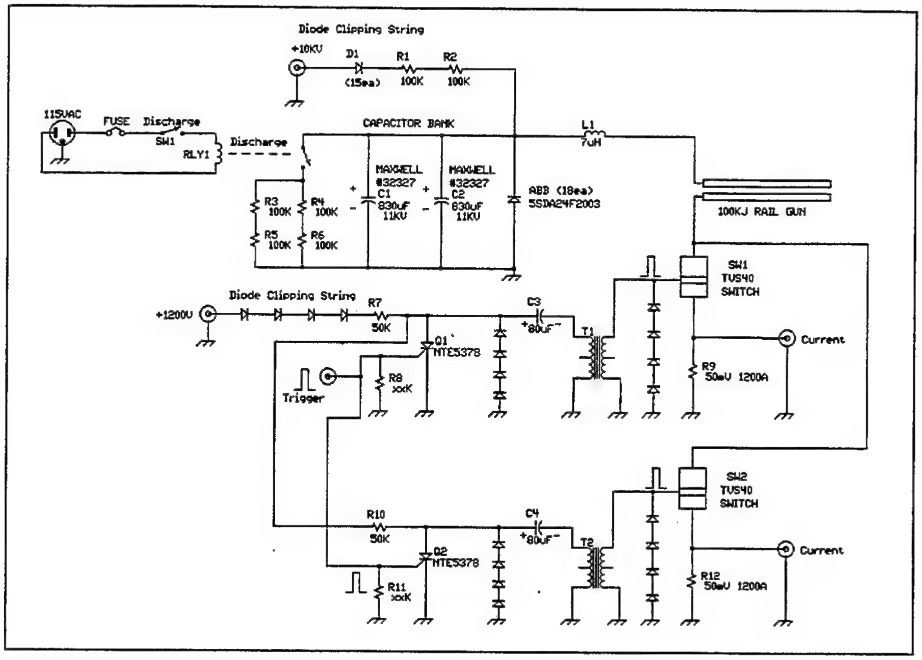

Figure 3.2 Railgun power unit schematic.

To meet the goal of accelerating masses of several grams and various configurations to high velocity a higher capacity power source was required. To this end, Maxwell Model 32327 capacitors were selected. Two 830μf, 10kV capacitors connected in parallel provide up to 100kJ of energy.

A coil is connected in series with the capacitors for pulse shaping. It has a measured inductance of 7μH and a resistance of about 0.9 mΩ. Maximum currents on the order of 100-200kA are expected, so the current limiting components were identified. These are the TVS-40 vacuum switch, rated at a peak current of 100 kA and the avalanche diodes, which have a limiting load integral of $4.2 \times 10^6 A^2s$, [12] translating to an operational threshold as shown in Fig. 3.3.

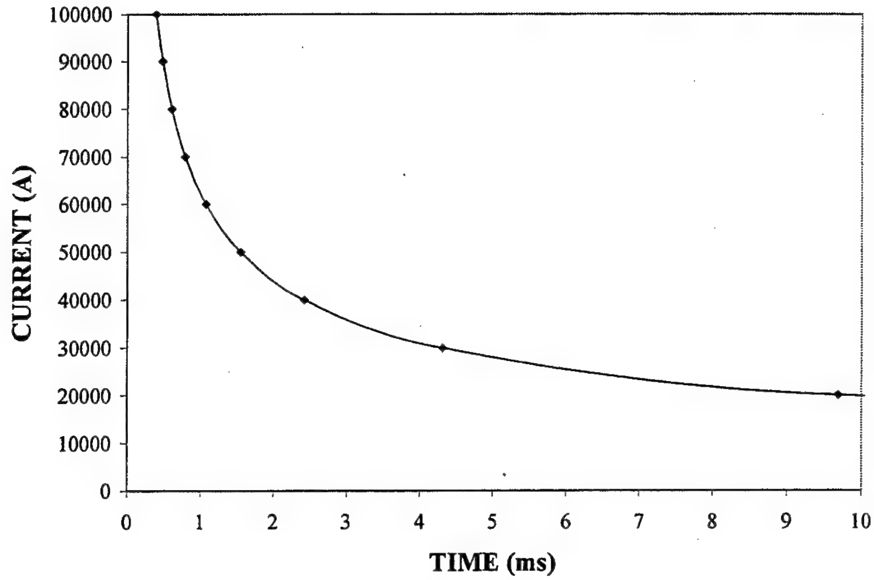

Figure. 3.3 Avalanche Diode Limiting Load. For safe operation the current pulse through the diode should not exceed this threshold.

To overcome these limitations and provide a safe power unit able to operate at full current capability, parallel switches and diode strings are incorporated in the power unit design.

Power unit components and support circuitry are enclosed in a wheeled metal cabinet, Fig. 3.4, which provides air-cooling and mobility.

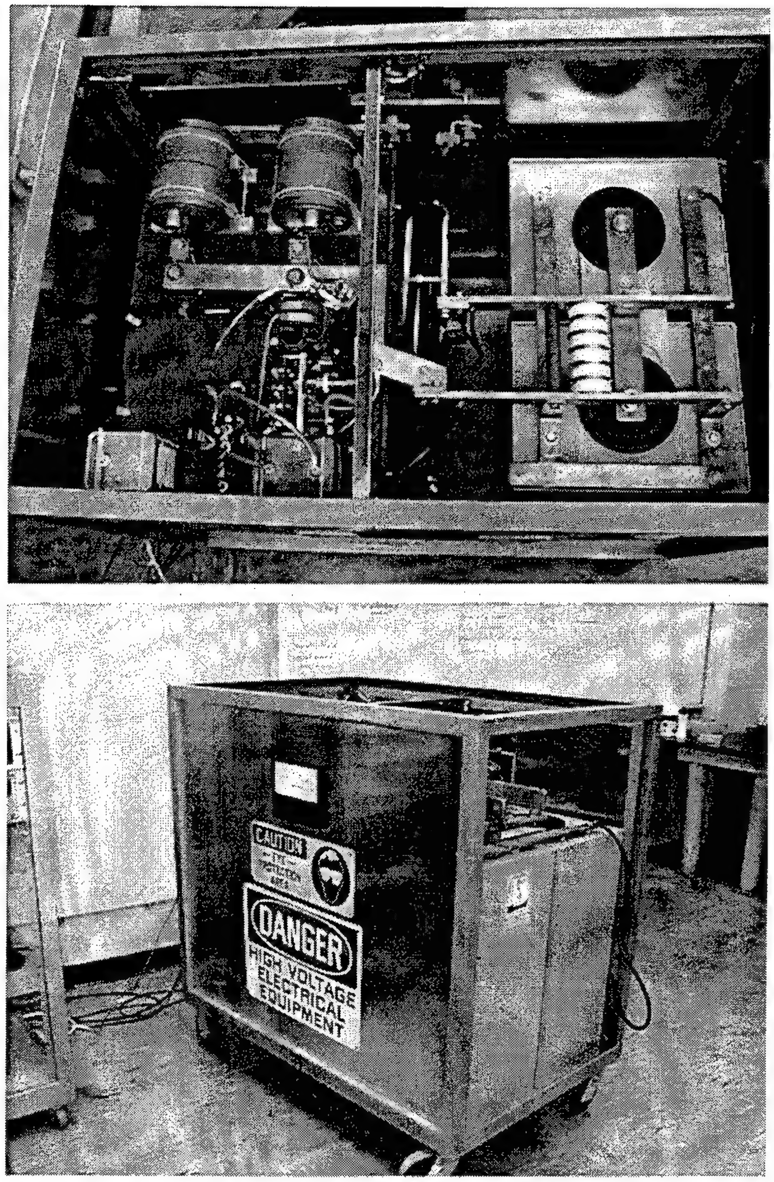

Figure 3.4 Power unit cabinet.

B. LAUNCHER DESIGN

The 1.2-meter railgun, Fig. 3.5, was designed to be easily expandable to allow experimentation with various bore sizes and rail configurations. It incorporates series trans-augmentation rails. The sandwich configuration, Fig. 3.6, makes component

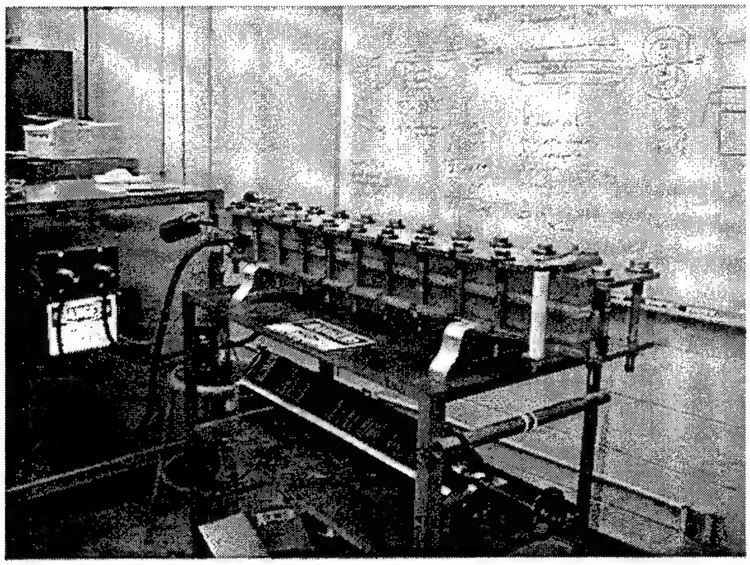

Figure 3.5 Railgun launcher.

fabrication relatively simple and inexpensive. It also provides excellent rail support and bore stability.

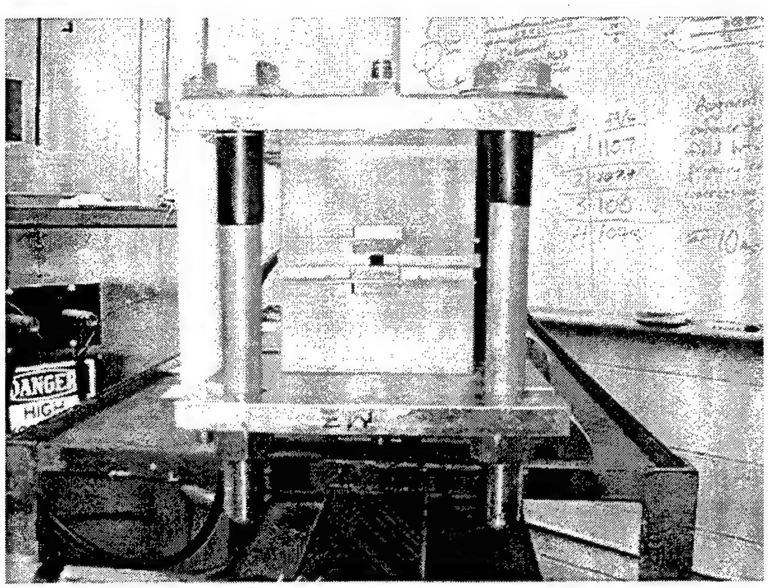

Figure 3.6 Railgun “sandwich” configuration.

The railgun support structure provides great strength and stiffness to oppose bore growth during firing. The brass cap plates are slotted to allow quick removal of the locking bolts for easy disassembly. Insulators break electrical contact between bolts and the metal clamping plate to reduce eddy currents. The details of the structural design can be found in Appendix A.

It is desirable to introduce the armature and projectile to the railgun with a certain initial velocity so that the Lorentz force does not need to overcome static friction and to minimize localized rail surface heating. The mechanism from a paintball gun was adapted to this purpose.

The paintball gun barrel was discarded and replaced by a square chamber matching the bore size and mounted in a threaded nylon bushing which secured the gun mechanism to the breach block, Fig. 3.7. The paintball gun mechanism uses a CO_2 cylinder and is triggered remotely with a solenoid switch. Qualitative testing of the gun

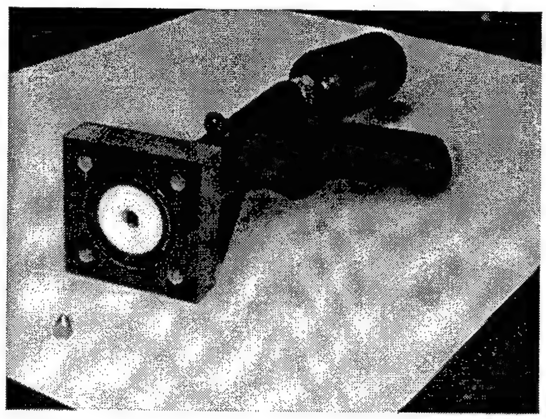

Figure 3.7 Paintball gun mechanism adapted for projectile injection.

mechanism with the square chamber, firing a projectile of several grams, proved satisfactory.

Detail drawings used during component fabrication and assembly are found in Appendix B.

C. PROJECTILE DESIGN

The severe bore erosion and pitting, Fig 3.8, common to railguns has been attributed to arc and plasma formation [13]. Moreover, the formation of plasma arcs in a railgun bore has been shown to reduce electrical efficiency significantly compared with a solid metal contact [14].

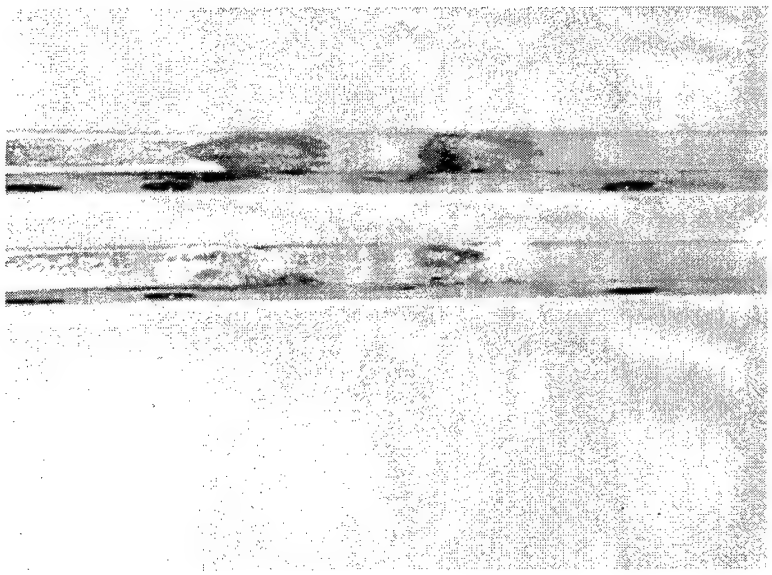

Figure 3.8 Rail damage due to arcing and plasma.

It is, therefore, desirable to use a sliding solid metal contact armature and to delay the inevitable transition to an arcing armature.

The occurrence of arcing within the bore has been attributed to melting of armature material due to ohmic heating at the rail-armature interface [13]. This melting leaves a gap between the rail and armature and promotes plasma formation and arcing.

Aluminum is the most common solid armature material. It is a good conductor, with relatively low density. It is easily machined and inexpensive. Unfortunately, it has a low melting temperature (660°C).

The melted aluminum also causes problems when it recondenses on the rail surfaces. After a few firings, aluminum buildup on the rail surfaces becomes significant and degrades performance.

Remedies to the melting problem are choosing an armature material with a higher melting point or choosing an armature configuration which slows the evolution of maximum temperature [13].

Molybdenum is an alternative armature material with a very high melting temperature (2625°C). It is unlikely molybdenum will melt in this railgun, regardless of geometry.

Less desirable characteristics of molybdenum are density about three times that of aluminum and poorer conductivity. It is also difficult to machine, flaking badly in the sample we have. Molybdenum is also more expensive than aluminum.

The initial armature design, shown in Fig. 3.9, is essentially a homogeneous molybdenum slug, being both armature and projectile. It is made of molybdenum and weighs a nominal three grams. Though the armature has a pointed nose, no attempt was made to stabilize it for atmospheric flight. It is intended for in-bore dynamic research.

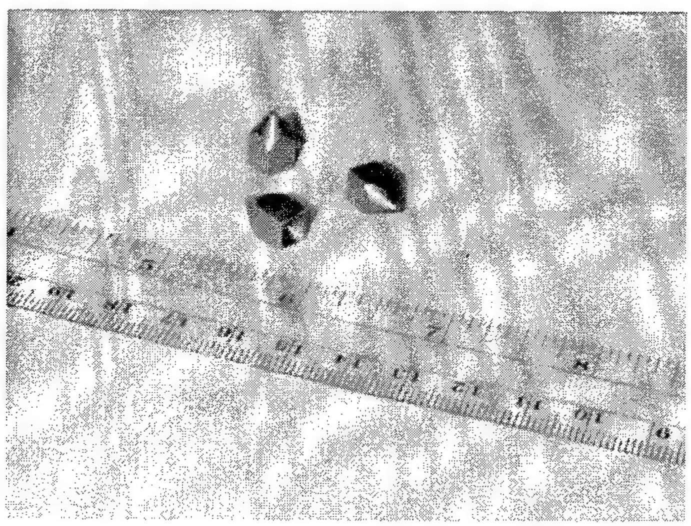

Figure 3.9 Initial railgun armature.

IV. OPERATIONAL PERFORMANCE

A. ELECTRICAL TESTING

Data collection for the most important railgun operating parameter, current, is accomplished with the Pearson Model 1330 wide band current monitor, Fig. 4.1.

Figure 4.1 Pearson current monitor.

Mounted with the main power return cable through its center, the monitor provides a voltage output with proportions of 5mV/A. This output was displayed on a Tektronix DSA 602A digitizing signal analyzer after passing through a 20dB attenuator.

Discharge of the power unit into a known load allows characterization of the power unit. Initial electrical testing utilized a variable resistance dummy load, Fig. 4.2, made of a three foot stack of 4" x4" x ¼" thick graphite plates. Compression of these plates allows the resistance of the stack to be controlled.

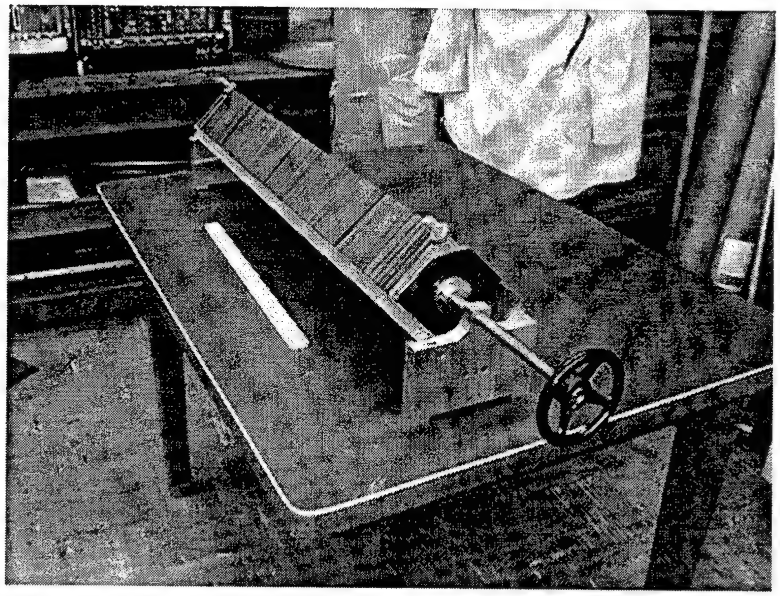

Figure 4.2 Dummy load.

The current curve of a 6 kV power unit discharge into the dummy load is seen in Fig 4.3. This compares closely with predicted power unit performance which is

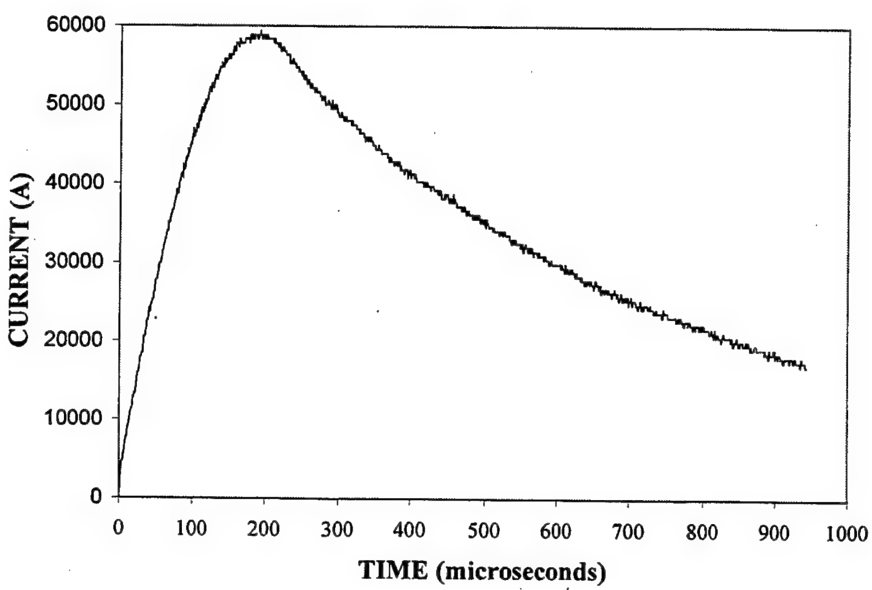

Figure 4.3 Railgun power unit discharge current.

described in detail in Appendix C.

The current rise time is 190μs. As this is a quarter period, C = 1660μf, and the period is $T = 2\pi\sqrt{LC}$, the overall power unit inductance is L = 9.3μH. Since, the capacitor inductances are small, about 0.04μH, this indicates about 2.3μH circuit inductance in the power unit in addition to the 7μH coil. The crowbar switch clamps after the current peaks, after which, the current fall off is proportional to $e^{-\frac{R}{L}t}$. Since a 50% current falloff occurs after 405μs, R is 15.92 mΩ. For this test the dummy load was set to15.00 mΩ, so the power unit resistance is about 0.92 mΩ.

One negative power unit performance characteristic noted during electrical testing was arcing between gaps in the power unit cabinet resulting from eddy currents induced by the inductor coil. This was observed when capacitor voltage exceeded 5 kV. Failure of the silicon controlled rectifier in the main power triggering circuit was attributed to these induced currents.

B. FIRING TESTS

Launcher pretesting occurred in two stages. First, the uniformity of electrical contact between the armature and rails was verified. Then the paintball gun injection mechanism was fired through the bore to confirm operation and to collect data for the firing circuit time delay.

Electrical contact verification was accomplished as follows. An ohmmeter was placed across the railgun power terminals. Then an armature was slowly pushed through the bore while the ohmmeter was monitored. The tightness of securing bolts was adjusted as required to provide good electrical contact without causing unnecessary friction between armature and rails. This adjustment proved more time consuming than anticipated due to the unevenness of the rail surfaces and the unyielding nature of the molybdenum projectile.

Once the bore verification was completed, an armature was inserted into the square chamber in the paintball mechanism. The armature was fired with the paintball mechanism. This procedure was repeated 10 times.

An average muzzle velocity of 30 meters per second was recorded with the Shooting Chrony Beta Model Chronograph. This was used to determine an estimated time required for the projectile to travel 30 centimeters down the bore. This time was 10 milliseconds. To provide time for the solenoid to actuate the paintball gun firing mechanism a time delay of 20 milliseconds was utilized.

The Stanford Research Systems Model DG535 digital delay pulse generator provided an initial trigger pulse to the solenoid followed 20 milliseconds later by a second trigger pulse to the power unit. Triggering of the TVS-40 vacuum switch was thereby delayed until the armature was at the appropriate place in the bore.

Initial firing tests with the molybdenum armature were conducted with a capacitor voltage of 4 kV. The firing circuit and power unit performed as anticipated. The firing discharge current curve is shown in Fig. 4.4. Projectile velocities between 17 and 30 m/s

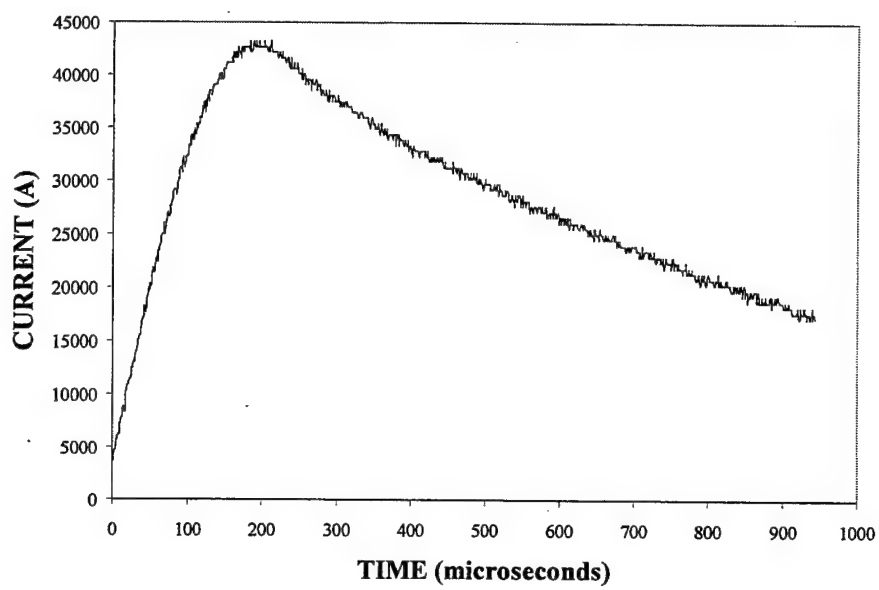

Figure 4.4 Railgun discharge current for 4 kV driving a 3g molybdenum armature.

were recorded. As this is comparable to the velocity expected from the CO_2 discharge alone, Lorentz force acceleration at this power level appears to have been insufficient to overcome surface friction. This presumption was supported when the projectiles and rails were examined, Fig. 4.5. The projectiles were undamaged but had a thick coating of

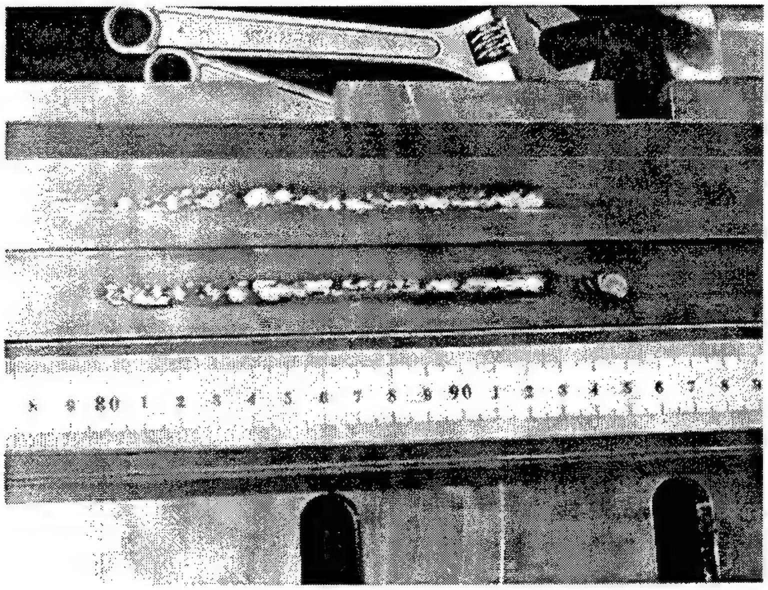

Figure 4.5 Armature and bore wear after 4 kV firing.

copper on the conducting surfaces. Likewise, the rails showed melting and pitting in the conduction path indicating high temperature arcing. Failure to achieve higher projectile velocity is now attributed to sticking of the Molybdenum armature to the copper rails.

The final firing attempt resulted in the projectile welding to the rails. The immobile projectile resulted in a longer than anticipated conduction pulse which exceeded the limiting load integral of the avalanche diodes. The crowbar circuit failed and further testing was curtailed.

C. CONCLUSIONS

A 1.2 meter railgun was designed, constructed and tested. Firing circuit, power unit, and launcher structure performed satisfactorily. In particular, the instrumentation

for measuring current pulse and velocity performed extremely well. Resumption of testing after crowbar circuit repair will support research into rail longevity issues, armature and projectile design, and railgun efficiency.

Crowbar circuit design should be revised to preclude the possibility of exceeding the diode limiting load integral. A TVS-40 vacuum switch based crowbar circuit may prove to be a better alternative to avalanche diodes. Though a TVS-40 would require more extensive circuitry, it may be less expensive. Performance testing with carbon projectiles should follow to prove launcher operation.

Once the crowbar circuit and launcher are performing as expected, alternative rail and armature materials should be tested. The ¼" square molybdenum projectiles, while durable, did not maintain electrical contact with the slightly variable bore size. Moreover, the tendency for copper to build up on the armature resulted in bore erosion and significantly increased the surface friction between the rails and armature. Trailing arm or U-shaped armatures may prove more capable of maintaining sliding contact with the inevitable bore size variation.

A material alternative for armatures worth exploring is metal-polymer combinations. Recently conventional small arms projectiles have been made of tungsten bonded in a matrix with polymers. Reported characteristics are density and hardness approaching that of tungsten but with the ability to deform under load and then return to their original size [17].

Reconfiguring the power unit to discharge the capacitors consecutively, at a predetermined interval, rather than simultaneously may provide a higher average current. Also, reduction or removal of the inductor coil should increase current for a given capacitor voltage and improve reliability due to the reduction of EM fields in the power unit cabinet. While removal of the inductor will shorten the pulse length is unlikely to impact performance significantly.

As experimentation with this railgun proceeds through higher power levels and to larger projectiles, a larger firing range will certainly be required.

APPENDIX A

RAILGUN LAUNCHER STRUCTURAL DESIGN

The structural design of the railgun launcher was based upon two requirements; strength and stiffness. The structure must be strong enough to contain any anticipated Lorentz force loading. Likewise, because solid metal contact armatures will be used the launcher structure must have sufficient stiffness to minimize bore growth due to loading.

Recalling (2.3) and (2.4), the longitudinal Lorentz force loading the rails can be expressed:

$$F = \frac{\mu_0 I^2 l'}{2\pi\, r} \tag{A.1}$$

where l' is rail length and r is the center to center distance between the rails. The distributed load is:

$$\frac{F}{l'} = W = \frac{\mu_0 I^2}{2\pi\, r} = \frac{(4\pi \times 10^{-7})(100000)^2}{2\pi(0.0127)}$$

$$W = 157400\,\frac{N}{m} = 17791\,\frac{lb}{in}$$

As the need for structural fasteners (bolts) spaced periodically down the length of the railgun is recognized, one can consider the interval between each pair of bolts as a beam supported at each end under a distributed load, Fig. A.1. Classic beam bending calculations can then be used to determine what bolt spacing is needed to achieve the stiffness required [16].

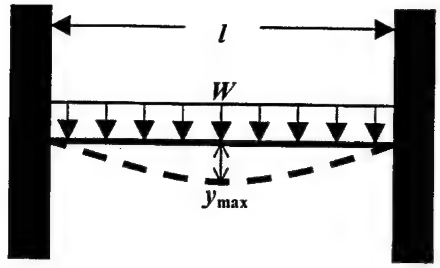

Figure A.1 Equivalent beam for calculations.

For this mode of beam bending the maximum beam deflection magnitude, $y_{\max}$ is expressed as:

$$y_{\max} = \frac{Wl^3}{384EI} \tag{A.2}$$

where l is the distance between the supports at each end of the beam, E is the modulus of elasticity of the beam and I is the rectangular moment of inertia of the beam. While this formula is quite straight forward, two elements of it are not. A maximum allowed deflection must be chosen and the rectangular moment of inertia for this non-homogeneous beam must be chosen.

Existing data reveals that an average copper railgun rail will have an overall surface variation, due to roughness and lack of flatness of 0.002 to 0.005 in [15]. Therefore, as negligible deflection is desired, $y_{\max} = 0.0002in$ is chosen.

The rectangular moment of inertia problem was more difficult to solve. The methods described in [16] were used. The railgun beam is a composite of copper rails, insulating materials and support structures. The equivalent homogeneous beam structure must be determined and its rectangular moment of inertia calculated. Beginning with the copper rails and phenolic insulation support structure maximum deflection was calculated. Rails and phenolic alone proved insufficiently stiff. Various structural augmentation configurations were evaluated, iterating through the deflection calculation until the optimum design was found.

The optimum composite beam configuration, Fig. A.2, had a 4" x 1-¾" phenolic block, (1), and 1-½" x ¼" phenolic spacers, (2) and (4), supporting 1" x ¼" copper rails, 3), all capped by a 6" x ½" brass plate, (5), for added stiffness. The brass plate was chosen due to being non-magnetic.

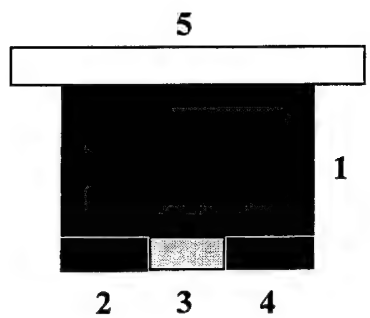

Figure A.2 Optimum composite beam configuration.

There are three steps which must be accomplished prior to solving a beam bending problem with a composite beam.

These are:

1. Determine the equivalent homogeneous beam.
2. Locate the centroid of that beam.
3. Determine the rectangular moment of inertia for the equivalent beam.

The equivalent homogeneous beam was calculated as if it was all phenolic. Thus, the non-phenolic components were converted to phenolic equivalents. This conversion is detailed below.

Phenolic: $E_p = 0.9 \times 10^6\, psi$

Copper: $E_c = 15.6 \times 10^6\, psi$

Brass: $E_b = 15.9 \times 10^6\, psi$

$$n_c = \frac{E_c}{E_p} = \frac{15.6}{0.9} = 17.3 \quad \text{and} \quad n_b = \frac{E_b}{E_p} = \frac{15.9}{0.9} = 17.67$$

The phenolic equivalents for the copper and brass components are found by multiplying the dimension perpendicular to the load, width, by the n factors above. So,

$$w_3' = n_c w_3 = (17.3)(1) = 17.3 inches$$

$$w_5' = n_b w_5 = (17.67)(6) = 106 inches$$

The equivalent beam, Fig. A.3, is made of three phenolic components. The top

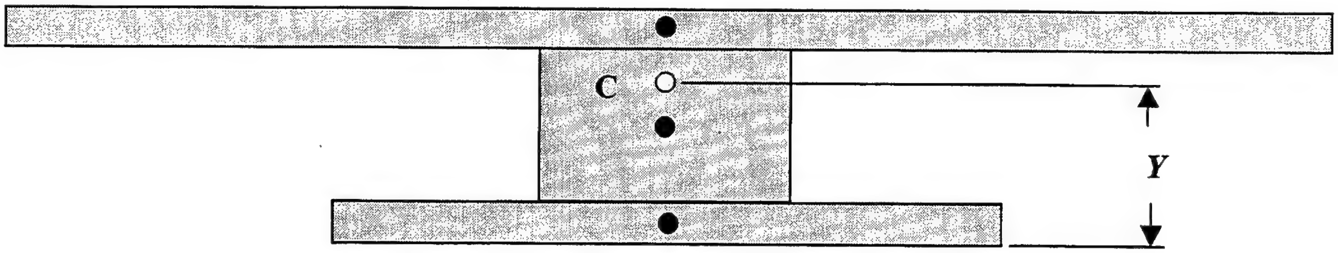

Figure A.3 Equivalent beam configuration. (lateral dimensions not to scale)

bar is 106" x ½", the center block is 4" x 1-¾" and the bottom bar is 20.3" x ½".

Now, the centroid of the equivalent beam must be found. From [16] we have, $Y\sum A = \sum yA$, where Y locates the centroid of the beam, A is the area of each beam component and y locates the centroid of each beam component.

	A (sq. in)	*y* (in)	*yA* (cu in)
1	53	2.5	132.5
2	7	1.375	9.625
3	10.15	0.25	2.54

So,

$$Y = \frac{(132.5in^3) + (9.625in^3) + (2.54in^3)}{(53in) + (7in) + (10.15in)} = \frac{144.665in^3}{68.56in} = 2.06 inches$$

The rectangular moment of inertia, I, from [16], is:

$$I = \sum (\tfrac{1}{12} bh^3 + Ad^2)$$

where b and h are the width and height of each beam component and d is the distance between y and Y.

$$I = \left[\tfrac{1}{12}(106in)(0.5in)^3 + (53in^2)(0.44in)^2\right] + \left[\tfrac{1}{12}(4in)(1.75in)^3 + (7in^2)(0.685in)^2\right]$$
$$+ \left[\tfrac{1}{12}(17.3in)(0.5in)^3 + (8.56in^2)(1.81in)^2\right] = 39.97in^4$$

Now, solving (A.2) for l:

$$l = \left[\frac{384(9x10^5\,psi)(39.97in^4)(0.0002in)}{17791\frac{lb}{in}}\right]^{\frac{1}{3}} = 4.99inches$$

For a railgun with an effective length of 48 inches, a minimum of 20 bolts would be required. Since the brass plate is 54 inches long 24 bolts were used with a center to center spacing of 4 5/8 inches.

Bolt size was determined to avoid exceeding the yield strength of the material and thus sustaining permanent deformation during axial loading. The yield strength for stainless steel is $YS = 42000ksi$. Considering the region between any four adjacent bolts, the individual bolt size is:

$$a = \frac{Wl}{4YS} = \frac{(17791\frac{lb}{in})(4.625in)}{4(42000psi)} = 0.49in^2$$

Since,

$$a = \tfrac{1}{4}d^2\pi$$

$$d = \sqrt{\frac{4a}{\pi}}in = 0.79in$$

The nearest standard bolt size, ¾ inch, was selected.

APPENDIX B
DESIGN DRAWINGS

This section contains the engineering drawings used in the construction of the railgun launcher and power unit.

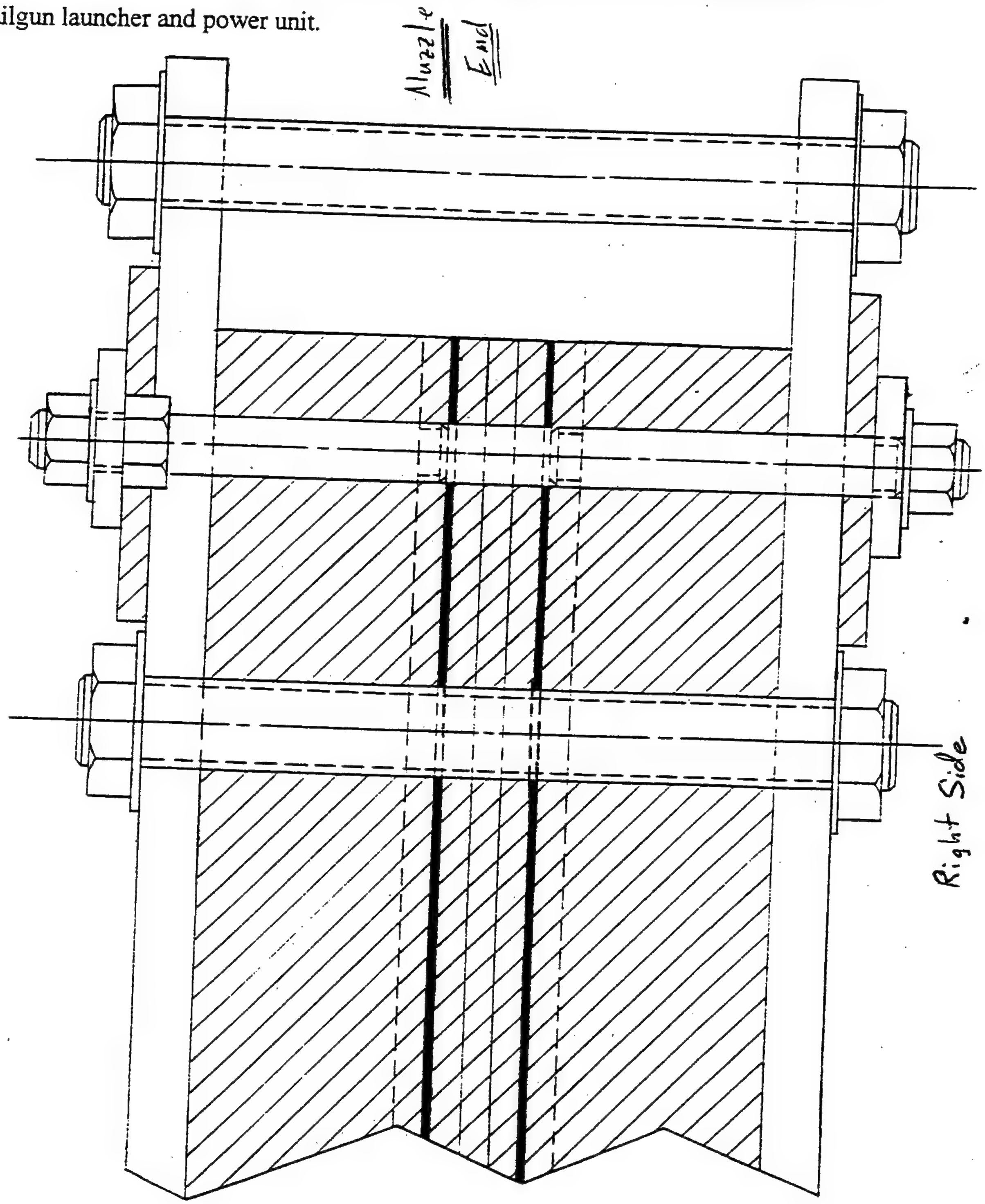

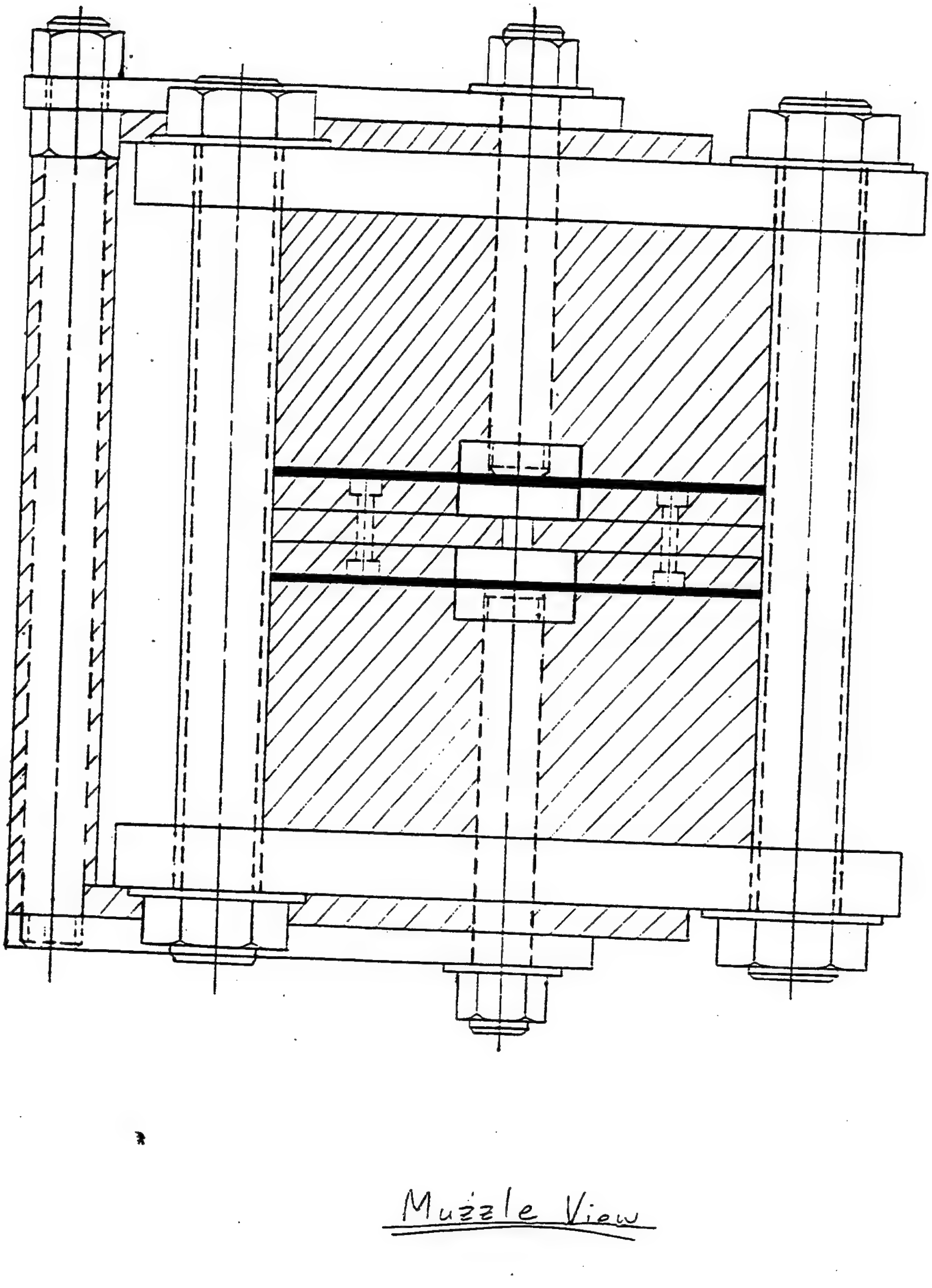

Muzzle View

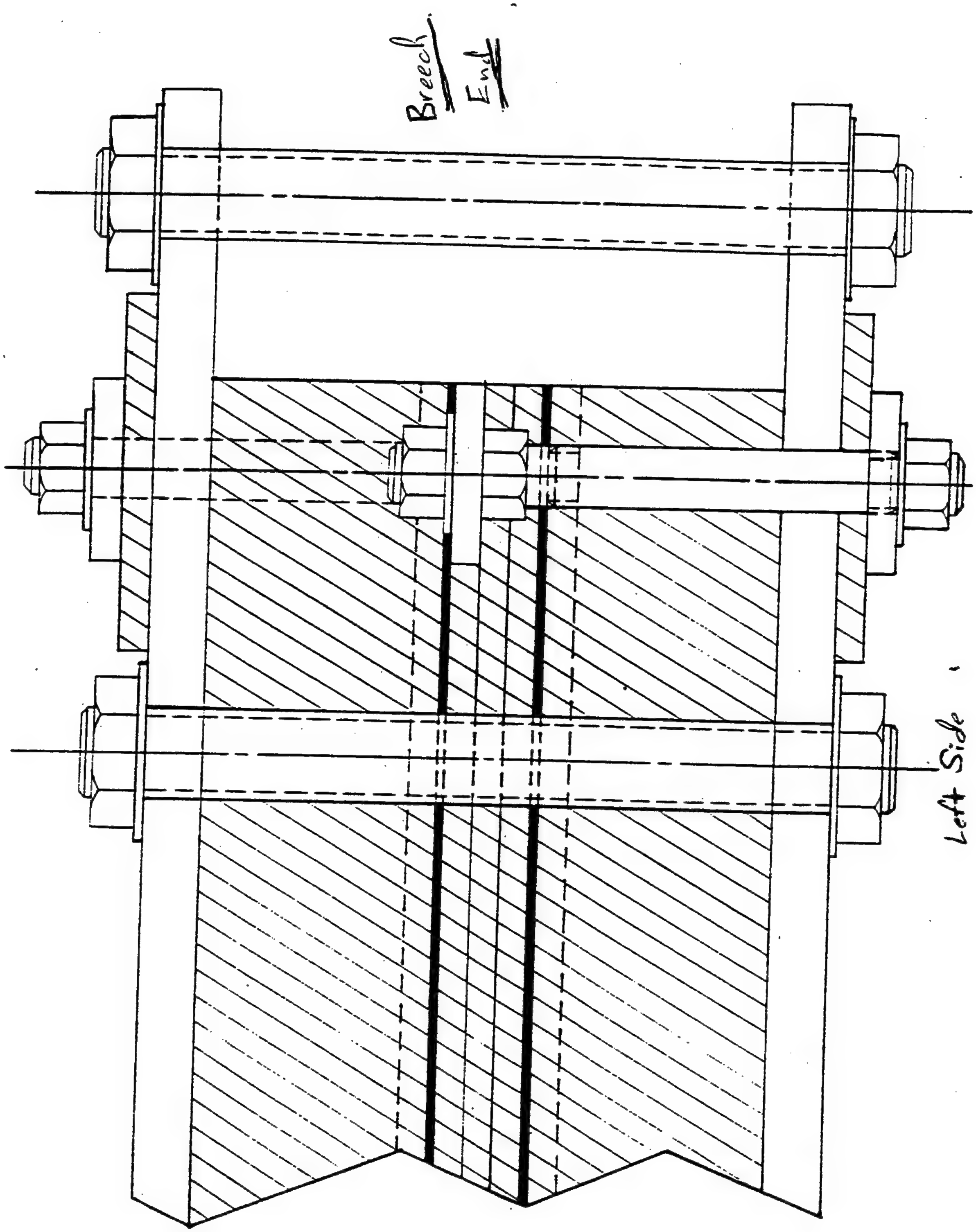
Breech End
Left Side

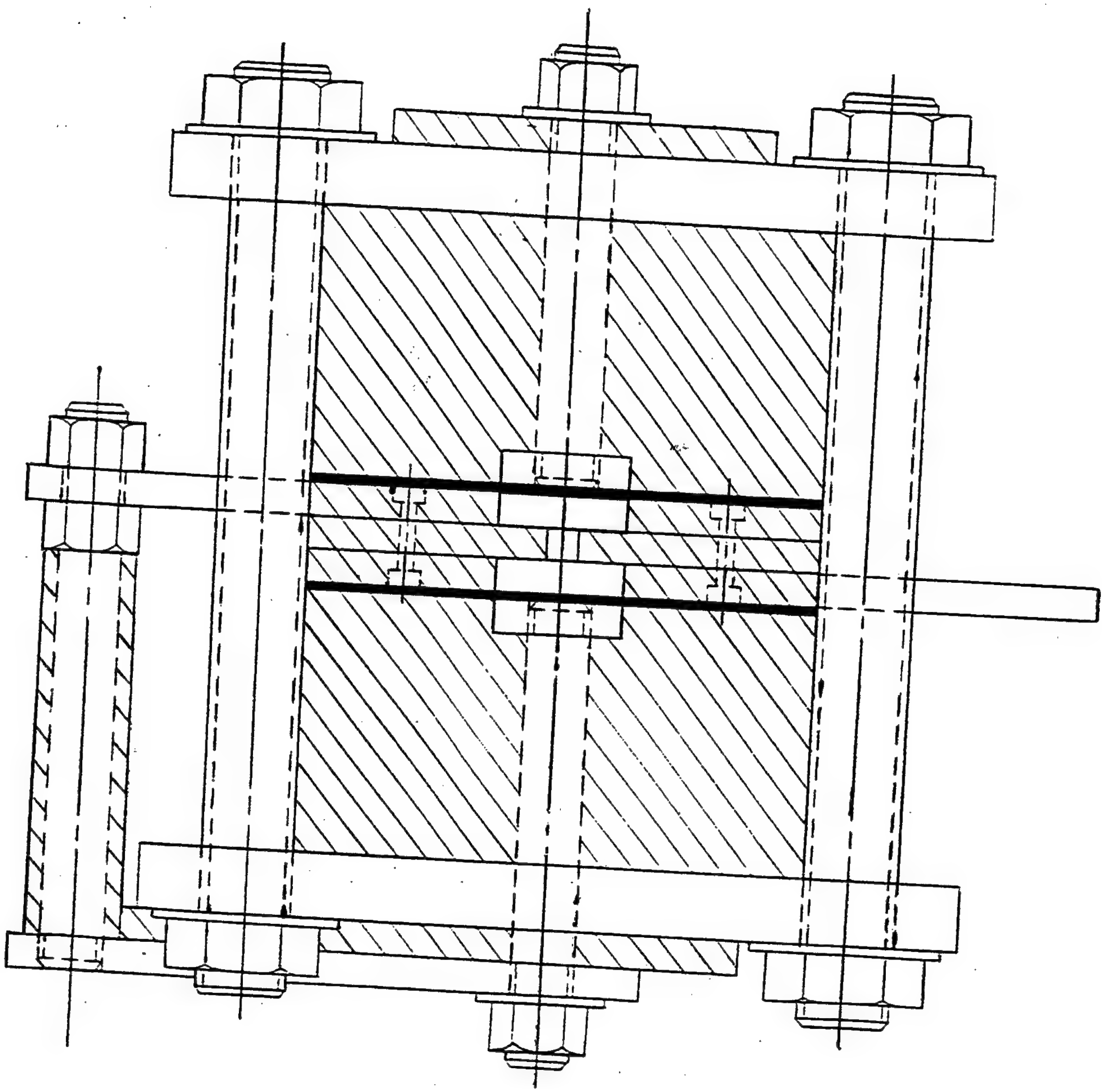

Breech View

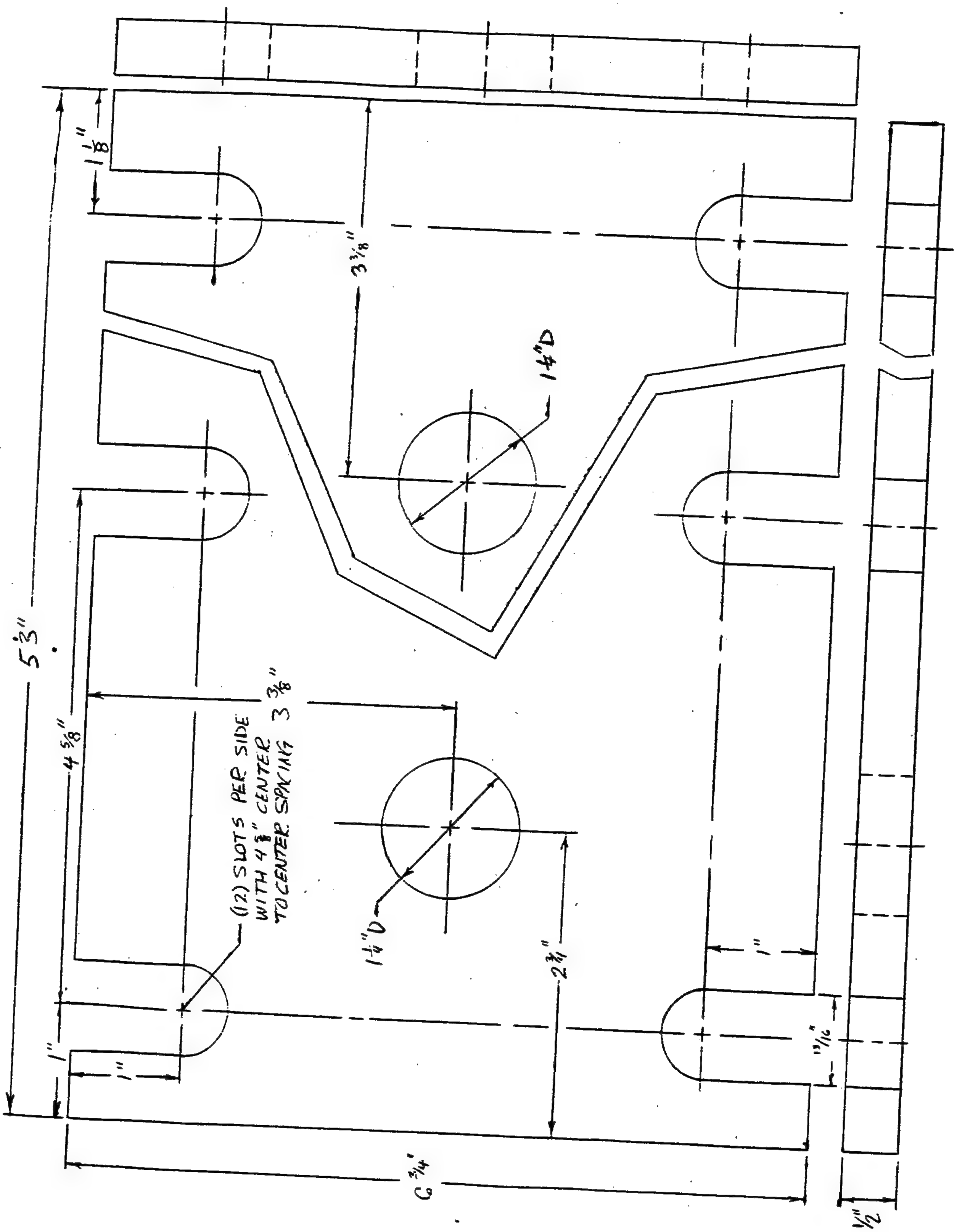
(12) SLOTS PER SIDE
WITH 4 5/8" CENTER
TO CENTER SPACING
5 3/4"
1 1/8"
3 3/8"
1 1/4"D
4 5/8"
3 3/8"
1 1/4"D
2 3/4"
1"
1"
1"
13/16"
6 3/4"
1/2"

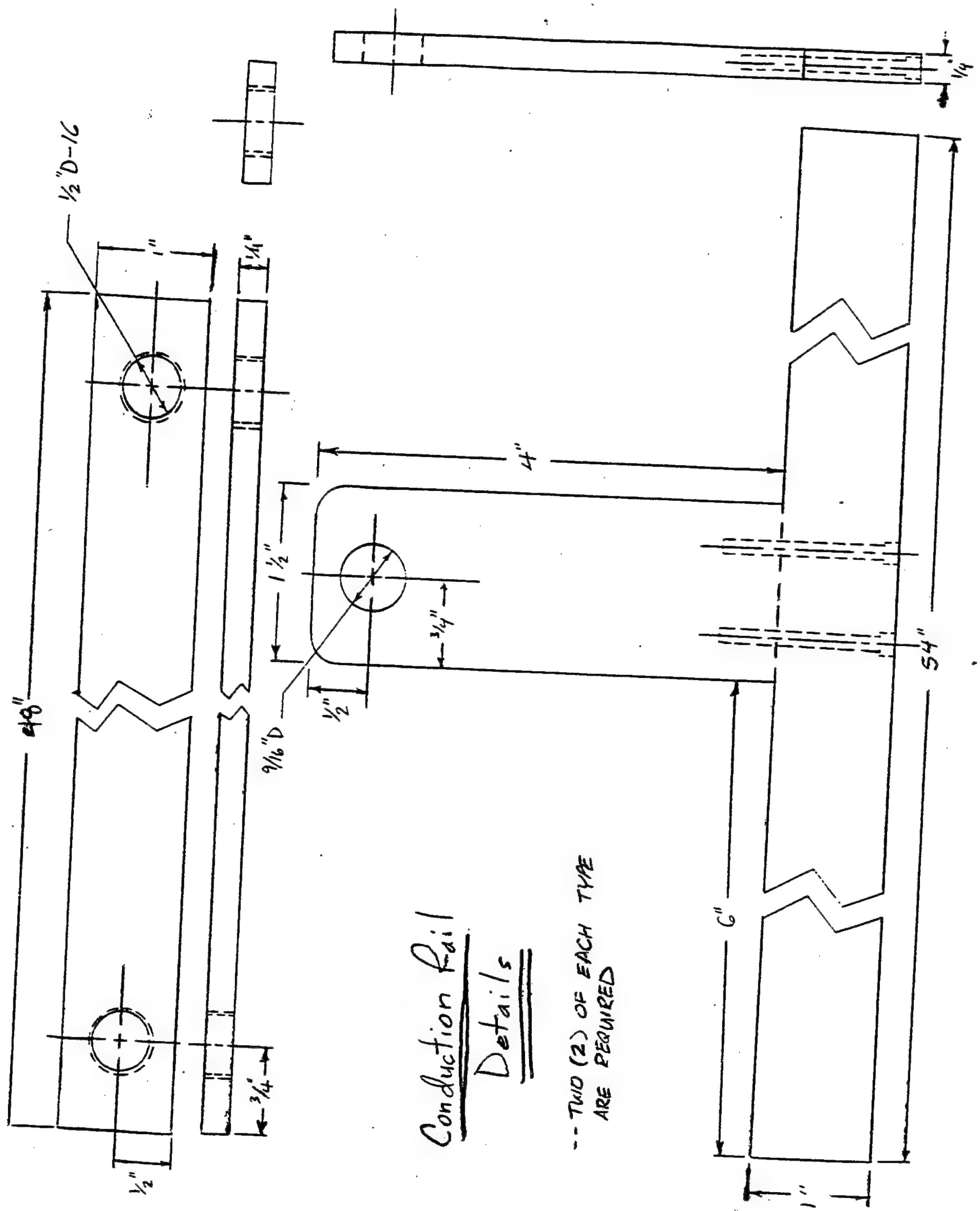
Conduction Rail
Details
-- TWO (2) OF EACH TYPE
ARE REQUIRED
48"
1/2"D-16
1"
1/4"
3/4"
1/2"
4"
1 1/2"
3/4"
1/2"
9/16"D
6"
54"
1"
1/4

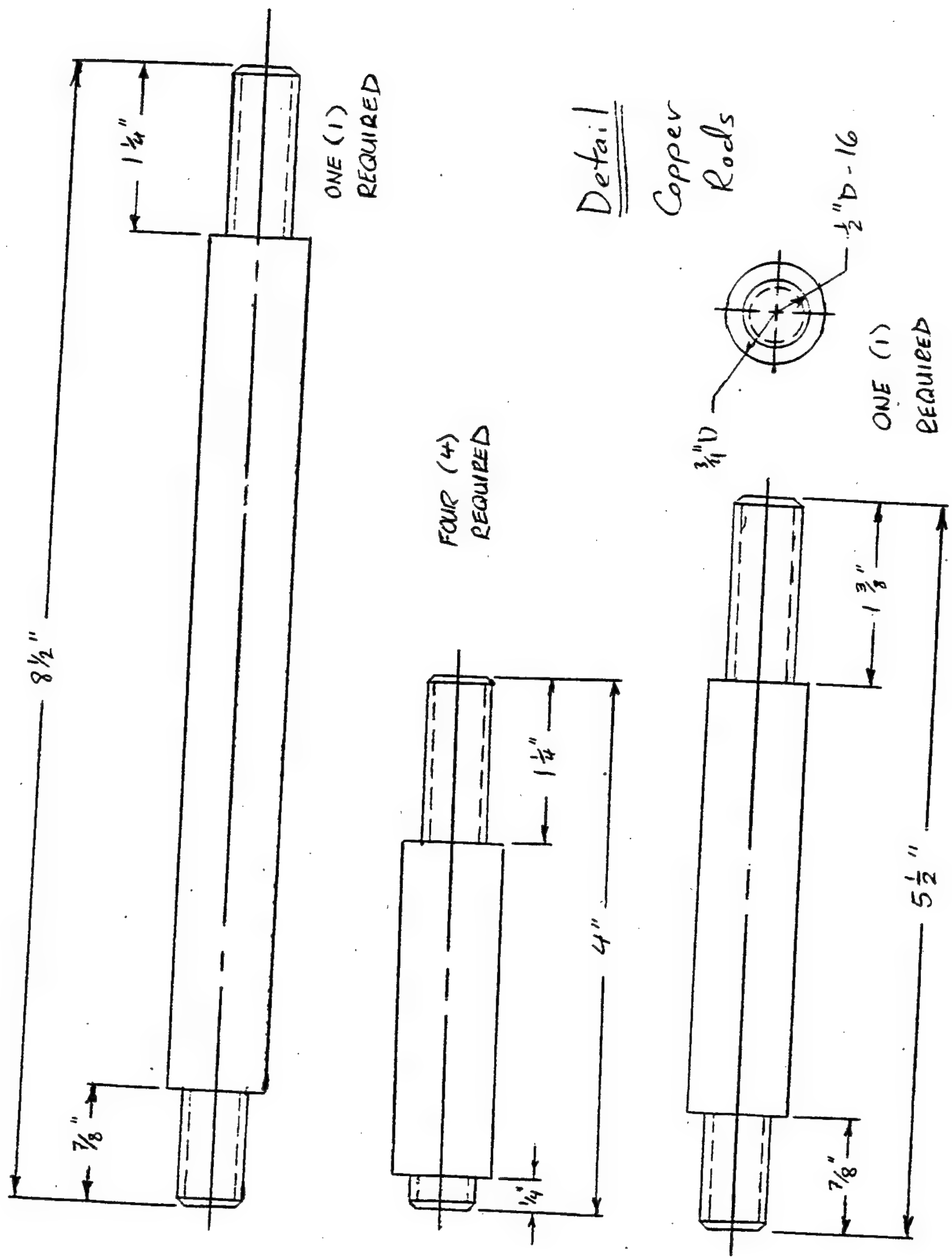
Detail
Copper Rods
ONE (1) REQUIRED
FOUR (4) REQUIRED
ONE (1) REQUIRED
8½"
1¼"
⅞"
4"
1¼"
¼"
5½"
1⅜"
⅞"
½"D-16
¾"D

Breech Block Assy

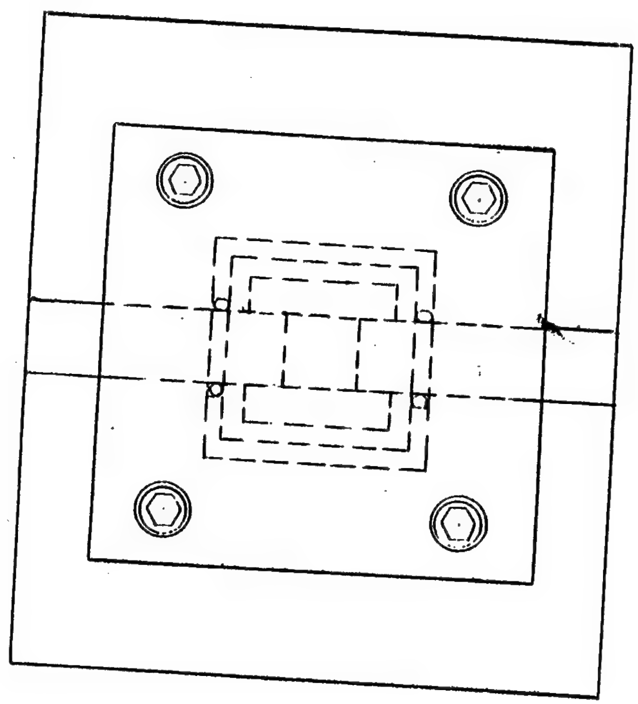

½" Square Bore

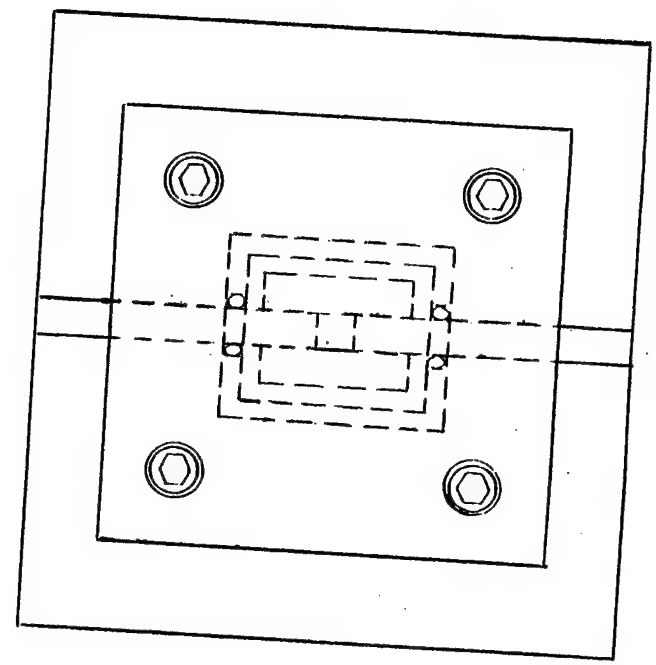

¼" Square Bore

Breech Block

End Cap

(Phenolic)

TYPE	1	2
A	1/2"	3/8"
B	2"	2 1/4"
C	7/8"	3/4"
D	1"	1 1/2"

ONE (1) EACH OF TYPES 1 + 2

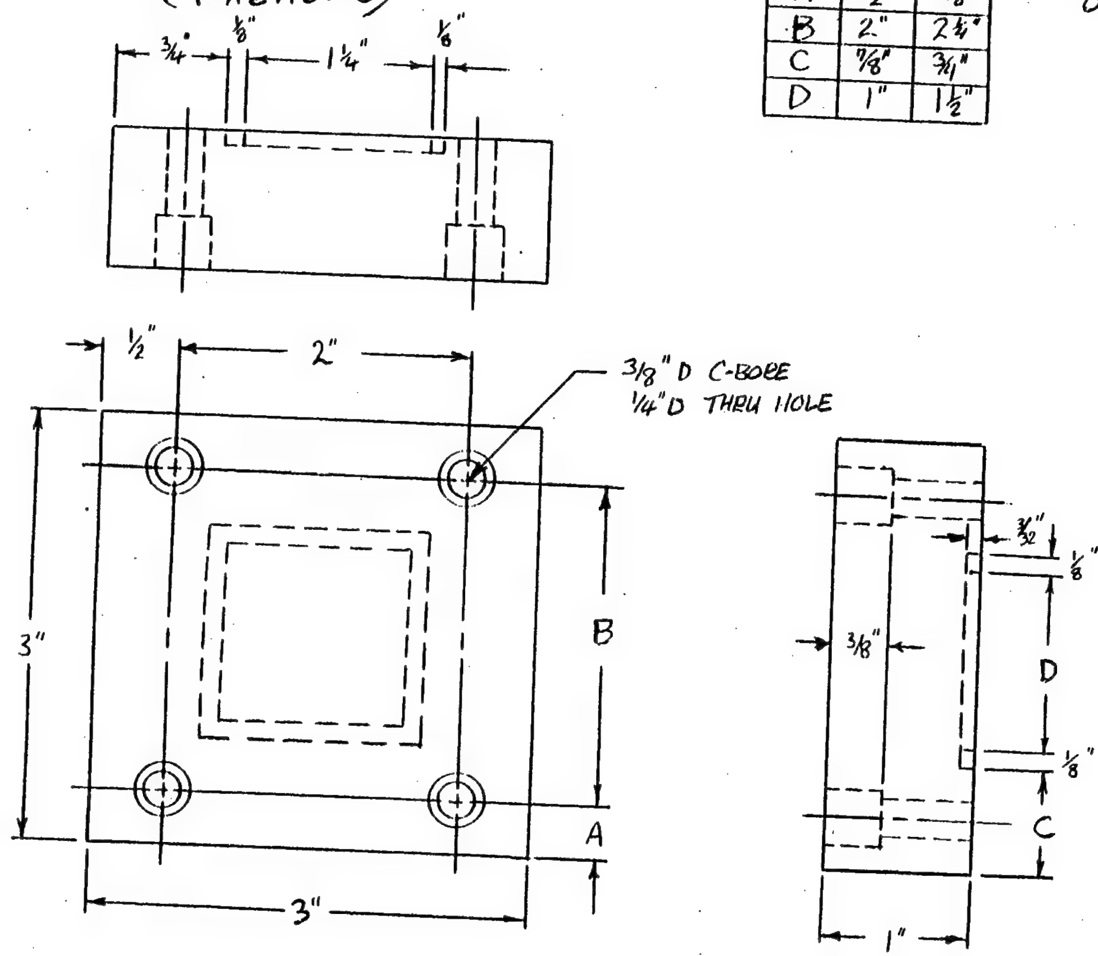

Breech Block
(Phenolic)

TWO (2) REQUIRED

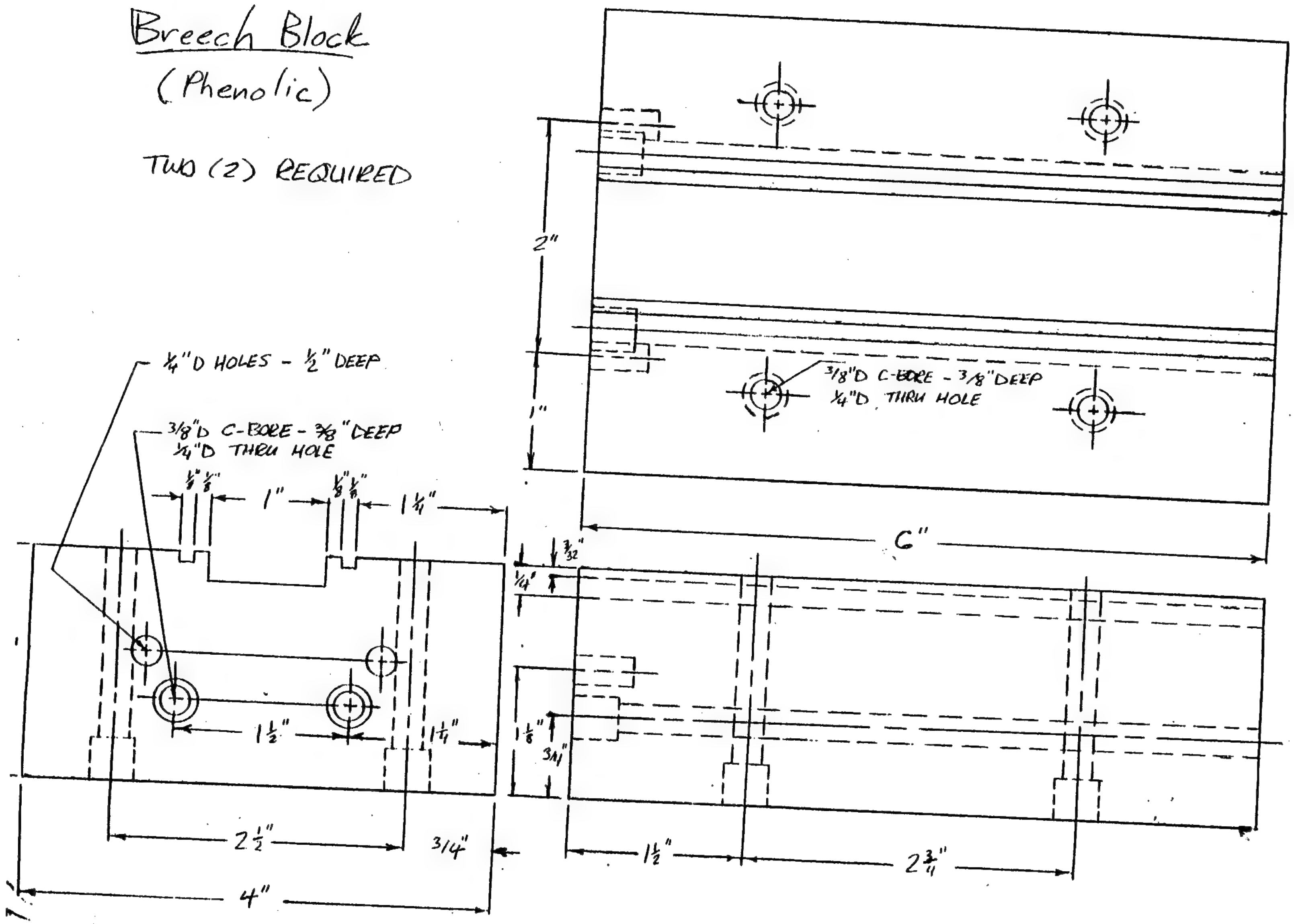

APPENDIX C
PERFORMANCE SIMULATIONS

This section contains the circuit configuration and simulation results used to predict power unit performance. The simulations were made using *MicroSIM Eval8*, which is an electrical engineering circuit design program. Note, that in the circuits, diode strings are simulated with timed switches as the software did not support the use of high voltage avalanche diodes.

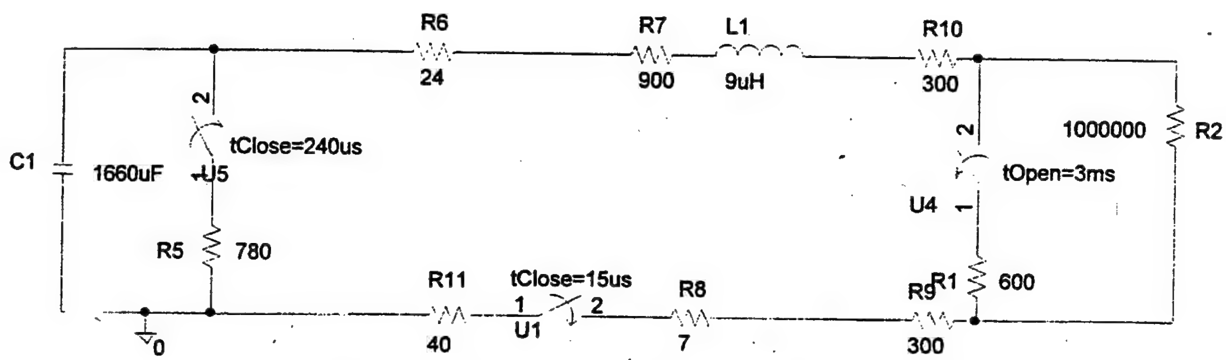

FIGURE C.1 INITIAL RAILGUN CONFIGURATION:
VOLTAGE: 5000 V
ONE DIODE STRING CROWBAR CIRCUIT
(ALL RESISTANCES IN MICRO OHMS)

(A) FIGURE C.2 INITIAL CONFIGURATION - 5000V - 1 DIODE STRING

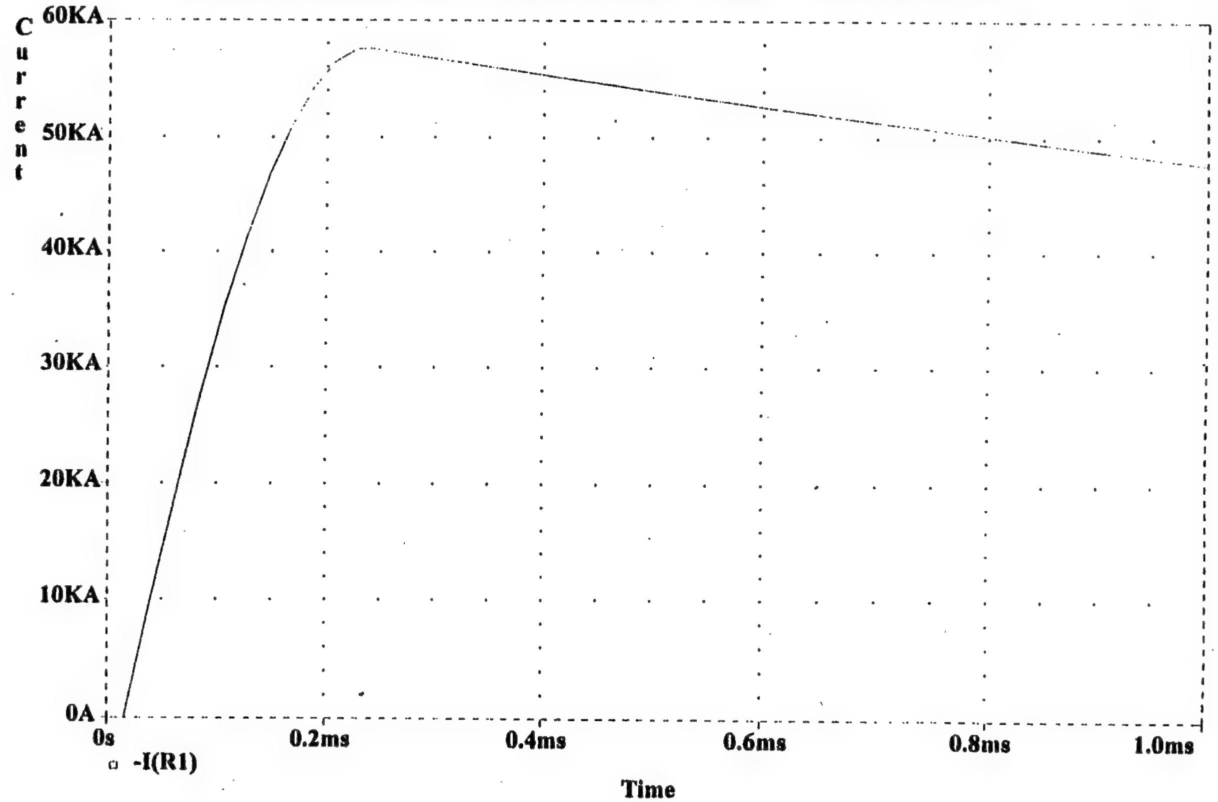

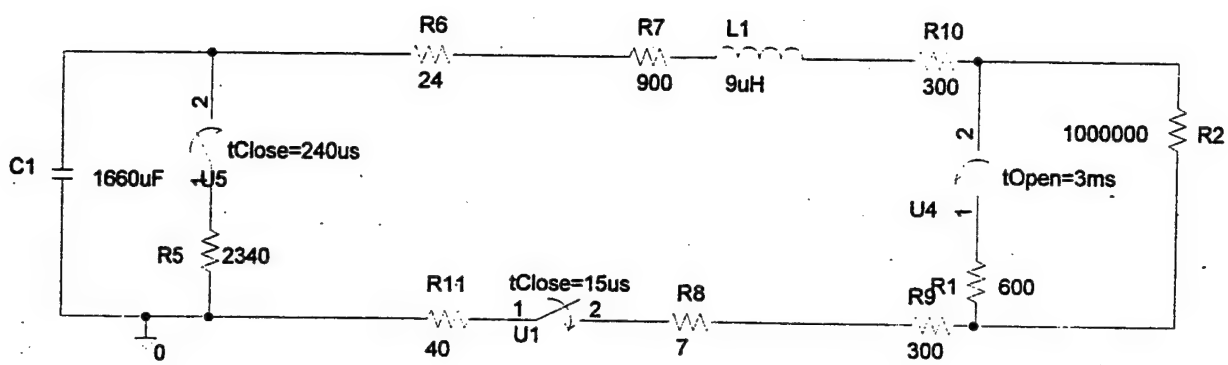

FIGURE C.3 INITIAL RAILGUN CONFIGURATION:
VOLTAGE: 10000 V
THREE DIODE STRING CROWBAR CIRCUIT
(ALL RESISTANCES IN MICRO OHMS)

(A) FIGURE C.4 INITIAL CONFIGURATION - 10000V - 3 DIODE STRINGS

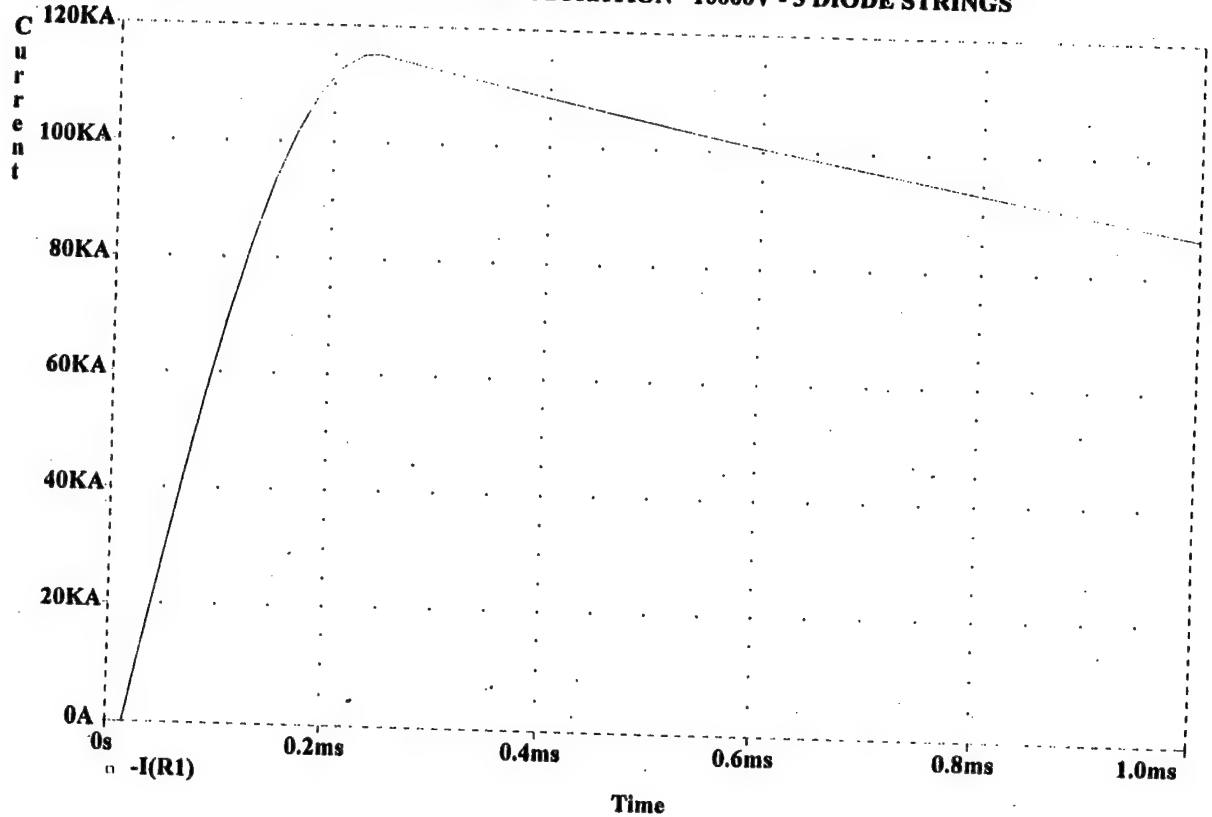

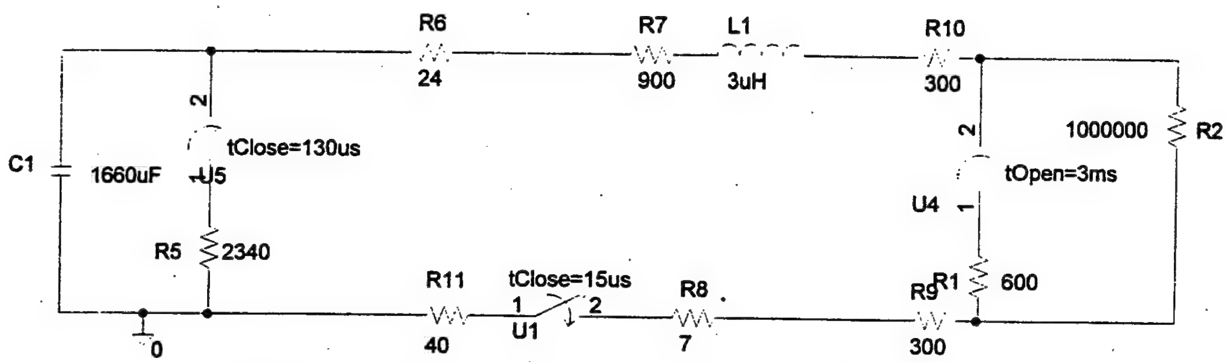

FIGURE C.5 REDUCED INDUCTANCE CONFIGURATION:
VOLTAGE: 10000 V
THREE DIODE STRING CROWBAR CIRCUIT
(ALL RESISTANCES IN MICRO OHMS)

(A) FIGURE C.6 REDUCED INDUCTANCE CONFIGURATION - 10000V - 3 DIODE STRINGS

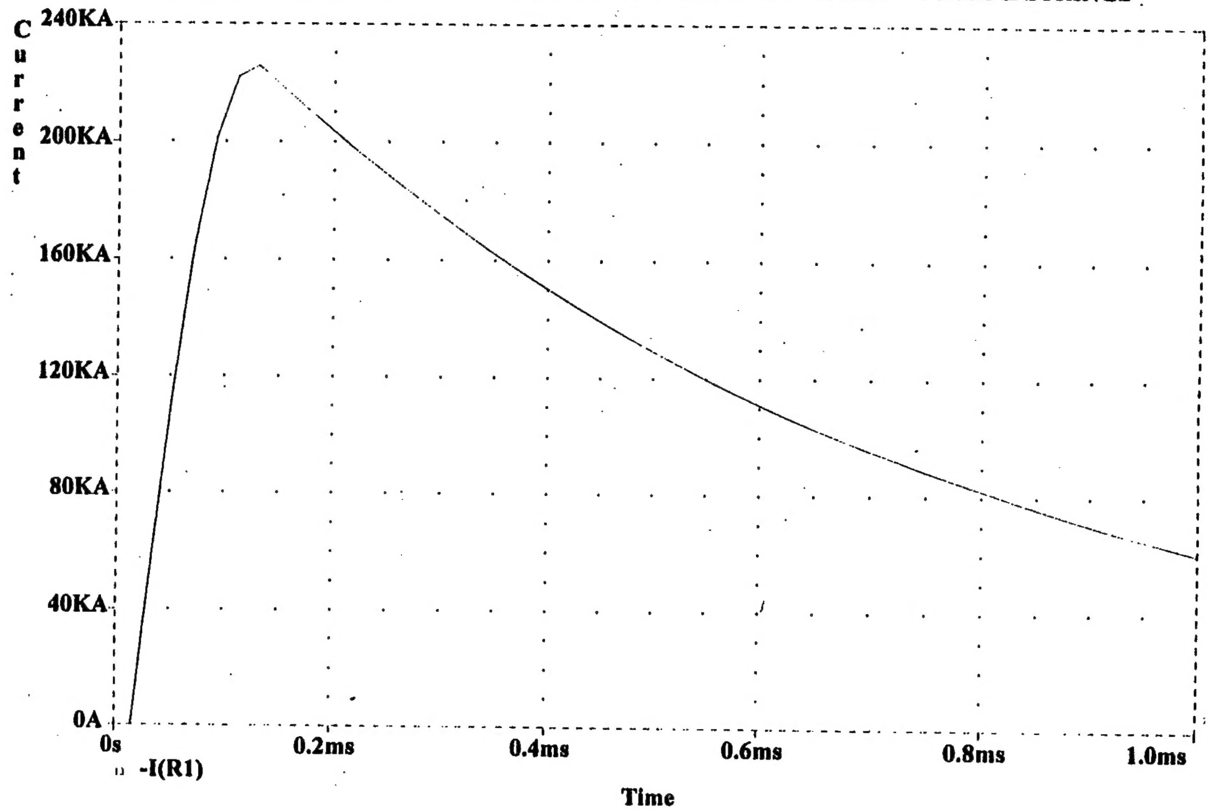

LIST OF REFERENCES

1. Fair, H.D., *Electromagnetic Propulsion: A New Initiative*, IEEE Transactions on Magnetics, Vol. Mag-8, No. 4, pp. 4-6, 1982.

2. McNab, I.R., *Early Electric Gun Research*, IEEE Transactions on Magnetics, Vol. 35, No. 1, pp. 250-261, 1999.

3. Rashleigh, S.C. and Marshall, R.A, *Electromagnetic Acceleration of Macroparticle to High Velocities*, Journal of Applied Physics, Vol. 49, No. 4, pp. 2540-2542, 1987.

4. Fair, H.D., *Application of Electric Launch Systems*, IEEE Transactions on Magnetics, Vol. 29, No. 1, pp. 342-344, 1993.

5. Center for Naval Analysis Report CRM 98-74, *Railgun Technology Assessment*, by Kohlberg, I. and Bomse, pp. 3-15, 1998.

6. Morison, S.L., *Lack of Naval Surface Fire Support Capability causes undue risk to U.S. Troops*, Navy News and Undersea Technology, p.4, May 10, 1999.

7. Hartke, J.P., *Characterization and Magnetic Augmentation of a Low Voltage Electromagnetic Railgun*, Master's Thesis, Naval Postgraduate School, Monterey, California, December 1997.

8. Lawrence Livermore National Laboratory Energy and Technology Review, *Hypervelocity Railgun Experiments*, p. 3, June 1980.

9. Walls, W.A., Weldon, W.F., Pratrap, S.B., Palmer, M., Adams, D., *Application of Electromagnetic Guns to Future Naval Platforms*, IEEE Transactions on Magnetics, Vol. 35, No. 1, p. 262, 1999.

10. Harold, E., Bukiet, B. and Peter, W., *Maximum Projectile Velocity in an Augmented Railgun*, IEEE Transactions on Magnetics, Vol. 30, No. 4, p. 1433, 1994.

11. Beach, F., *Design and Construction of a One Meter Electromagnetic Railgun*, Master's Thesis, Naval Postgraduate School, Monterey, California, June 1996.

12. ABB Semiconductors AG Document No. 5SYA 1131-01, *Avalanche Rectifier Diode 5SDA 24F2303*, July 1998.

13. Schooldermann, A.J., deZeeuw, W.A. and Koops, M., *Electrothermal Design Aspects of Transitioning Solid Armatures*, IEEE Transactions on Magnetics, Vol. 29, No. 1, p.865, 1993.

14. Bauer, D.P., *Achieving High Efficiency with Conventional Railgun Launchers*, IEEE Transactions on Magnetics, Vol. 31, No. 1, p. 263, 1995.

15. Knoth, E.A. and Bauer, D.P., *Armature Contact Load Dynamics*, IEEE Transactions on Magnetics, Vol. 31, No. 1, p. 201, 1995.

16. Beer, F.P. and Johnston, E.R., *Mechanics of Materials*, pp. 150-175, McGraw-Hill Book Co., 1981.

17. Brezny, L.P., "Kent Cartridge Tungsten-Matrix Ammunition," *Wildfowl*, v. 14, pp. 17-19, February 1999.

INITIAL DISTRIBUTION LIST

1. Defense Technical Information Center.. 2
   8725 John J. Kingman Rd., STE 0944
   Fort Belvoir, VA 22060-6218

2. Dudley Knox Library... 2
   Naval Postgraduate School
   411 Dyer Rd.
   Monterey, CA 93943-5101

3. Professor William B. Maier II, Code PH/Mw....................................... 10
   Department of Physics
   Naval Postgraduate School
   Monterey, CA 93943-5000

4. Professor Andres Larraza, Code PH/La... 1
   Department of Physics
   Naval Postgraduate School
   Monterey, CA 93943-5000

5. Engineering and Technology Curriculum, Code 34................................. 1
   Naval Postgraduate School
   700 Dyer Rd., Rm 115
   Monterey, CA 93943-5107

6. LT Michael R. Lockwood.. 2
   53 Third Ave.
   Rochester, NY 14612